NUREG/CR-1674
EGG-2058
Distribution Category: R3

FISSION PRODUCT RELEASE FROM LWR FUEL FAILED DURING PCM AND RIA TRANSIENTS

Daniel J. Osetek
John J. King

Published October 1980

EG&G Idaho, Inc.
Idaho Falls, Idaho 83415

Prepared for the
U.S. Nuclear Regulatory Commission
Washington, D.C. 20555
Under DOE Contract No. DE-AC07-76IDO1570
FIN No. A6041

ABSTRACT

The fission product release from light-water-reactor-type fuel rods to the coolant loop during four design basis accident tests conducted in the Power Burst Facility is presented. One of the tests was a power-cooling-mismatch test in which a single fuel rod was operated in film boiling beyond failure. The other three tests were reactivity initiated accident tests, in which the fuel rods were failed as a result of power bursts resulting in radial average peak fuel enthalpies of 250, 260, and 350 cal/g. Measurements of short-lived fission products by on-line gamma spectroscopy and important aspects of fission product behavior observed during the tests are discussed. Time-dependent release fractions for short-lived fission products are presented and compared with release fractions suggested by the Reactor Safety Study, NRC Regulatory Guides, and measurements from the Three Mile Island accident. Iodine behavior observed during the tests is discussed, and fuel powdering as a source of particulate fission product activity is suggested as a previously neglected aspect of accident analysis.

SUMMARY

Accurate description of fission product behavior during normal and accident situations is recognized as an important aspect of reactor safety. An understanding of fission product behavior is essential to the definition of accident source terms, and to the specification of fuel conditions that prevail in a reactor core during irradiation or following an accident. The primary objective of the Power Burst Facility (PBF) fission product studies is to experimentally investigate fission product behavior under accident conditions.

Fission product behavior was monitored during four light water reactor (LWR) fuel performance tests conducted in the in-pile loop of the PBF, located at the Idaho National Engineering Laboratory. One of these tests (Test PCM-1) was a power-cooling-mismatch (PCM) test during which a single pressurized-water-reactor-type fuel rod was operated in film boiling until failure and for 400 s after failure. A substantial fraction of the fuel rod melted during the test, producing a fission product release indicative of failures more severe than simple cladding rupture. The other three tests included in this study (RIA-ST-1, RIA-ST-2, and RIA-ST-4) were reactivity initiated accident (RIA) tests during which LWR-type fuel rods were subjected to a range of power bursts producing different degrees of fuel rod damage and fission product release.

An advanced fission product detection system (FPDS) incorporating on-line gamma spectroscopy was added to the PBF to monitor fission product activity during fuel performance tests. The gamma spectrometer used in the FPDS is a specialized system designed and built by EG&G Idaho, Inc., to provide accurate monitoring over the wide range of fission product concentrations produced in the PBF test loop. The need for continuous measurement and fine resolution of changes in fission product concentration during normal operating conditions and during the simulated accident conditions are requirements that had to be met by an advanced design. Gamma spectra acquired during the four tests were analyzed to determine the relative concentrations of identifiable fission products, and the relative release fraction histories were developed by comparison of the measured releases with the inventories calculated by the ORIGEN computer code.

Fission product behavior during the PBF tests is generally characterized by large noble gas release fractions, medium to high rubidium release fractions, low to medium iodine release fractions, and widely varying cesium, barium, and lanthanum release fractions. Noble gas isotopes demonstrated the largest release in Test PCM-1 and the RIA-ST-2 experiment, and ^{142}La exhibited the largest release during the RIA-ST-1 and RIA-ST-4 experiments. Iodine release fractions were very small, compared to the noble gas release fractions in the two tests that produced high fuel temperatures and large percentages of fuel melting (Test PCM-1 and RIA-ST-4). The other two tests (RIA-ST-1 and RIA-ST-2), which produced no evidence of fuel melting, showed larger fractions of iodine release relative to the noble gas releases. During RIA-ST-1, three different iodine isotopes each displayed a rapid and distinct drop in relative release fraction after equilibrium had been established. The change is attributed to an increased iodine loss coefficient as a result of changing loop coolant conditions. Several relative release fraction histories from the RIA-ST-4 experiment showed a monotic increase over an extended time period, indicating continuing fission product source terms.

The overall results of fission product release measured during the PBF tests show reasonably good agreement with the projections given in the Reactor Safety Study and NRC Regulatory Guides for noble gas and alkali metal release fractions. However, the halogen concentrations measured in the coolant were considerably lower in the PBF tests that included fuel melting; this effect may be attributable to early deposition of fission products on cladding or test train materials. The alkaline earth and refractory elements showed relatively high release fractions during the RIA tests. Possible explanations are the short irradiation times and the high fission rate near the fuel pellet surface characteristic of the RIA tests, and/or the extensive fuel fracturing and powdering that occurred during the tests.

The release fraction histories provide a detailed description of fission product behavior during the accident conditions simulated in the PBF tests, and illustrate the importance of time-dependent measurement and its application to accident analysis.

ACKNOWLEDGMENTS

The authors thank M. H. Putnam for her continued support in computer code development and modification, which has produced the relative release fraction plots displayed in this report. Special thanks are given to B. G. Schnitzler for the setup and running of the ORIGEN code that yielded the fuel rod inventories for this study. The gamma-ray data qualification and error analysis performed by C. M. McCullugh is also sincerely appreciated.

CONTENTS

FIGURES

TABLES

FISSION PRODUCT RELEASE FROM LWR FUEL FAILED DURING PCM AND RIA TRANSIENTS

1. INTRODUCTION

The risk associated with the operation of nuclear power plants has been assessed in several safety studies.[1-3] A recognized uncertainty in the risk estimates stems from the lack of data regarding release of radioactive material. With the exception of the Three Mile Island accident, which is still being investigated, little information has been provided about radiation source terms from reactor accidents. The bulk of information used for analyzing the consequences of accidents originates from out-of-pile experiments and conservative analytical estimates. The important aspects of fission product behavior include not only definition of the possible accident source terms, but also an understanding of the chemical and physical behavior of the radioactive fission products in reactor systems. A thorough understanding of this behavior and its dependence on the key fuel behavior parameters and coolant conditions will offer the opportunity to describe the fission product source terms, and thus the consequences, of postulated accidents.

In addition to providing accurate estimates of accident source terms, a thorough understanding of fission product behavior offers the possibility of interpreting reactor fuel conditions from on-line measurements of the appropriate fission product behavior parameters. If realized, the fuel condition monitor may prove to be a beneficial instrument for mitigating the deterioration of defective or damaged fuel and to help prevent the exacerbation of fuel damage accidents.

EG&G Idaho, Inc., is currently conducting reactor safety research experiments for the United States Nuclear Regulatory Commission.[4-5] The objective of this program is to define the behavior of light water reactor (LWR) fuel rods operated under normal and accident conditions. An important part of this program is concerned with evaluating fission product behavior during the fuel performance tests conducted in the Power Burst Facility (PBF).

This report summarizes the fission product behavior observed during four LWR fuel performance tests conducted in the in-pile loop of the PBF at the Idaho National Engineering Laboratory. One of these tests (Test PCM-1) was a power-cooling-mismatch (PCM) test during which a single PWR-type fuel rod was operated in film boiling until failure and for 400 s after failure. A substantial fraction of the fuel rod melted during the test, producing a fission product release indicative of failures more severe than simple cladding rupture. The other three tests included in this study (RIA-ST-1, RIA-ST-2, and RIA-ST-4) were reactivity initiated accident scoping tests (RIA-ST) during which LWR-type fuel rods were subjected to a range of power bursts producing different degrees of fuel rod damage and fission product release.

Section 2 of this report describes the PBF experimental facility and the fission product detection system (FPDS) used to monitor the radioactive fission products in the coolant of the test loop. Section 3 describes the design, conduct, and fuel behavior results of Test PCM-1, RIA-ST-1, RIA-ST-2, and RIA-ST-4. Fission product behavior observed during the four tests is summarized in Section 4 in terms of relative isotopic release fractions. Data from the four different tests are compared with fission product release data reported in the literature,[6] in NRC Regulatory Guides,[7,8,9] and in the Reactor Safety Study.[1] Conclusions regarding fission product behavior are discussed in Section 5, and a complete set of the isotopic release fraction histories is presented in Appendix A, provided on microfiche attached to the inside of the back cover.

2. EXPERIMENTAL FACILITY AND INSTRUMENTATION

The Power Burst Facility is a specialized test reactor designed to test nuclear fuel and components under off-normal operating conditions. Located at the Idaho National Engineering Laboratory, the PBF is operated by EG&G Idaho, Inc., for the U.S. Nuclear Regulatory Commission. This section describes the PBF and the associated fission product detection system (FPDS) used to obtain data on fission product behavior during these tests.

2.1 Power Burst Facility

The facility is made up of an open pool reactor which is used to drive the nuclear operation of test fuel in a separate in-pile coolant loop. Figure 1 is a cutaway view of the PBF reactor. The reactor core is a right-circular fuel annulus, 1.3 m in diameter and 0.914 m in length, with a centrally located test space (flux trap), 0.21 m in diameter. Nuclear operation is regulated by eight control rods for reactivity adjustment during steady state operation, and four additional transient rods to dynamically control the reactivity in the core during power burst operation. The PBF reactor can be operated in three modes: (a) a steady state mode with power levels up to 28 MW, (b) a natural power burst mode with a reactor period as short as 1 ms and peak power as high as 270 GW, and (c) a shaped burst mode to provide various energy densities in the test rod(s) for simulating many types of postulated reactor accidents.

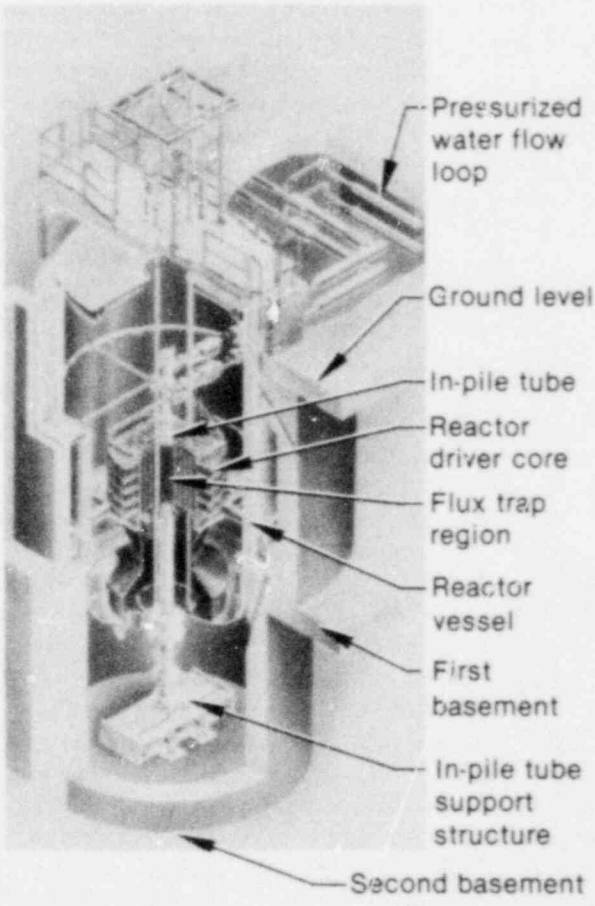

Figure 1. Cutaway view of the PBF reactor.

The PBF driver core is cooled by light water from a low pressure, two-loop coolant system. The experiments are mounted in an in-pile tube (IPT) and cooled by a separate high pressure coolant loop shown in Figure 2. The in-pile tube is a thick-walled, Inconel 718, high strength pressure tube designed to accommodate a pressure pulse of up to 51.7 MPa above the steady state pressure in the coolant loop system without damage to the driver core. A zircaloy-4 flow tube is positioned inside the IPT to direct the coolant flow. Coolant enters through an inlet nozzle at the top of the IPT above the reactor core and flows down the annulus between the IPT wall and the flow tube. It then reverses at the bottom of the flow tube and passes up through the test shroud to cool the test fuel rod(s). The coolant exits above the reactor core through the IPT outlet nozzle.

An experiment consists of one or more LWR-type fuel rods, 0.91 m in length, each mounted in individual coolant flow shrouds inside an instrumented test train. Test conditions are monitored by a variety of thermocouples, flowmeters, pressure transducers, and radiation detectors. The loop coolant system provides the experiment with water at pressures, temperatures, and flow rates typical of normal operation in a BWR or PWR and any off-normal conditions necessary to simulate a particular accident.

Fuel rods that fail as a result of testing, or rods that may be defective and allow fission products to leak from their interior, produce a fission product source term to the circulating coolant stream. A sample of the loop coolant is taken from a tap

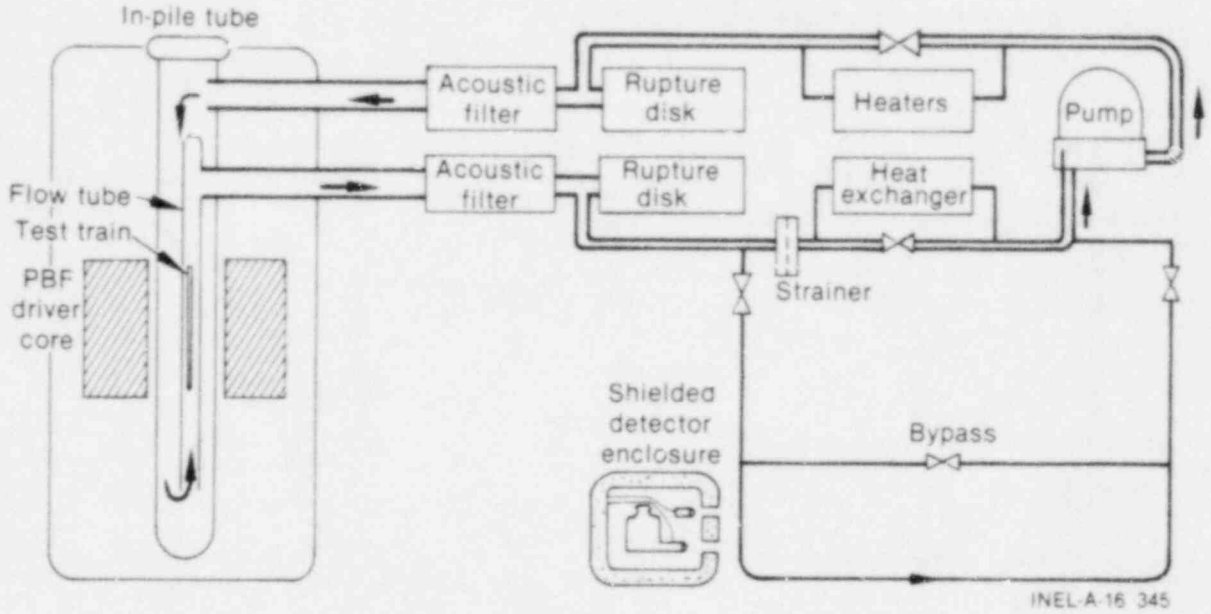

Figure 2. PBF loop schematic with FPDS sample line.

just upstream of the loop strainer and directed to the FPDS shielded detector enclosure in the second basement of the PBF. Flow through the sample line is proportional to loop flow, and typically runs between 0.006 and 0.032 L/s. The identity and quantity of radioactive fission products released from test fuel rods can be monitored simultaneously using the specialized on-line gamma spectroscopy techniques, described subsequently, to provide an indication of rod failure, the time of the rod failure, and concentration histories of the short-lived fission products within the loop coolant.

2.2 Fission Product Detection System

An advanced fission product detection system[10,11,12] has been developed that incorporates on-line gamma spectroscopy for monitoring fission product activity during fuel performance tests at the PBF. The FPDS is shown schematically in Figure 3. It consists of three basic subsystems: a sodium iodide (NaI) gross gamma detector, a delayed neutron (DN) monitor, and a germanium detector-based gamma spectrometer. The gross gamma and delayed neutron monitors are typical commercial equipment, but the gamma spectrometer is a unique, specialized system designed and built by EG&G Idaho, Inc., to provide accurate monitoring over the wide range of fission product concentrations produced in the PBF test loop. Continuous measurement and fine resolution of changes in fission product concentration during normal operating conditions and during simulated accident conditions required an advanced design. A detailed description of the PBF fission product detection system is given in Reference 12.

Some of the capabilities included in the FPDS are:

1. High resolution gamma spectra
2. Precision constant electronic energy calibration
3. High count rate capability
4. Remote control, six-position collimation
5. Continuous monitoring
6. Minimum spectrum acquisition time of 15 s
7. Automatic or operator-controlled data acquisition
8. Optional on-line spectra analysis.

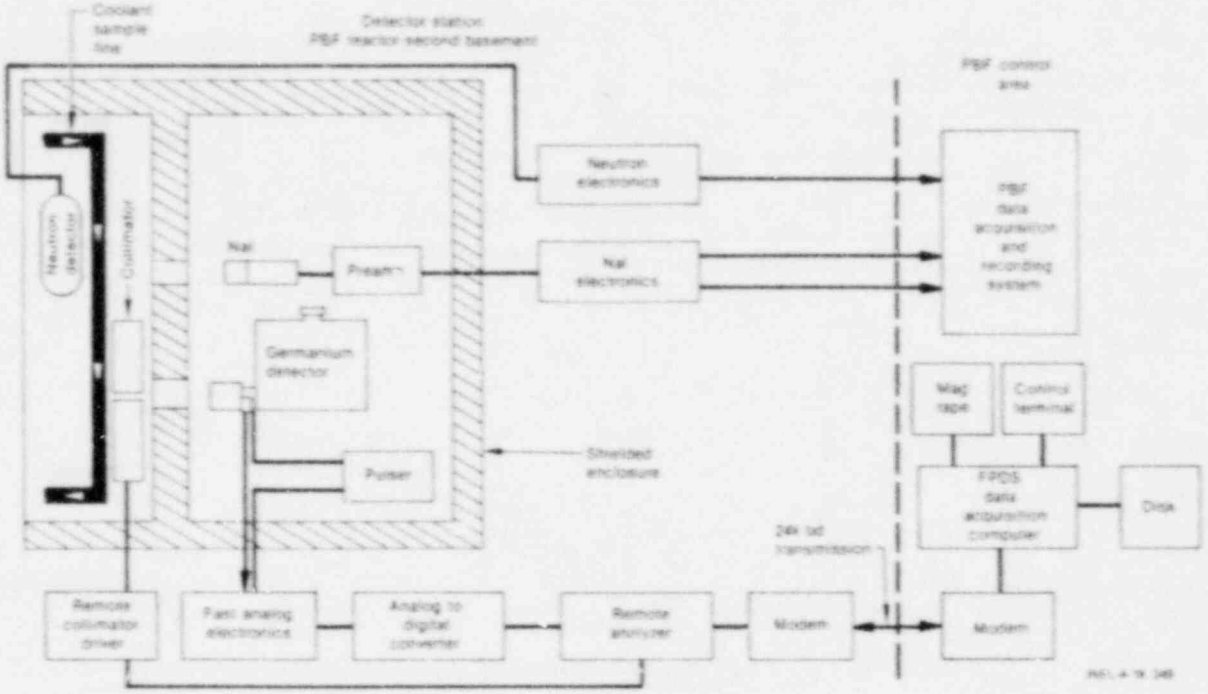

Figure 3. Schematic diagram of FPDS instrumentation.

Although high resolution is a feature expected in any commercial system, the PBF system maintains this excellent resolution at count rates in excess of 100 000 counts per second (cps). The combination of fast analog electronics and a remote controlled variable aperture collimator helps ensure monitoring capability over the wide range of gamma flux presented to the system. During extreme conditions, system dead time may approach 90%, but the 10% live time remaining permits acquisition of useful fission product information when conventional systems would saturate. The electronic calibration is maintained by a precision pulser that provides stable reference pulses to simulate fixed gamma ray pulses that are collected and stored along with each spectrum. Continuous monitoring is a necessary feature to ensure recording of rapid changes in fission product concentration. This is accomplished by using a dual memory, remote microprocessor. While one memory is acquiring a fresh spectrum, the other is transmitting a previously acquired spectrum to a recording device. The 15-s limitation on minimum spectrum acquisition time is dictated by the transmission and recording time. When fission product concentrations in the coolant are low and spectra acquisition times are longer than 300 s, on-line analysis of each spectrum is possible using the main data acquisition computer. When spectra are acquired rapidly, analysis is deferred until after the test.

Using sophisticated computer routines,[13] each spectrum is processed to determine the type of fission products present in the sample line. Then, by comparison with the system calibration data, the concentration of each identified isotope is calculated. The various fission product release quantities are determined by multiplying the concentrations by the loop coolant volume, and the release fractions are derived by comparison with the calculated inventories of each isotope. The computer code ORIGEN[14] is used to generate the appropriate fission product inventories for each test.

3. FISSION PRODUCT RELEASE TESTS

A series of fuel performance tests is being conducted in the PBF to study the behavior of LWR fuel rods during various postulated reactor accidents. During some of the more severe tests, the fuel rods experience significant damage, resulting in large fission product releases. Four of the tests that included fuel rod failures offered an opportunity to evaluate the behavior of several short-lived fission products released to the coolant.

One of the tests in this group of four was a power-cooling-mismatch test (PCM-1) designed to investigate the behavior of a single PWR-type fuel rod during high power operation in film boiling. The other three tests in the group of four were reactivity initiated accident tests, two of which were designed to simulate a hypothetical control rod ejection accident in a commercial BWR (RIA-ST-1 and RIA-ST-2) and one of which was designed to simulate a PBF accident (RIA-ST-4).

A brief summary of the design, conduct, and results of these four tests is given below; a detailed description of each test can be found in References 15 through 20. Fission product behavior for each of these tests is discussed in Section 4. The relative isotopic release fractions are given in Appendix A.

3.1 Test PCM-1

The objectives of Test PCM-1 were to evaluate the behavior of a PWR-type fuel rod subjected to high temperature film boiling operation for a time beyond failure, with large local regions of molten fuel providing the potential for energetic molten fuel-coolant interaction upon failure.

Film boiling can occur when fuel rod power is sufficiently increased without an accompanying increase in coolant flow rate, or by a reduction in coolant flow rate without a comparable decrease in rod power. Film boiling degrades the heat transfer from the fuel rod, causing an increase in operating temperatures and the possibility of cladding and fuel melting.

The single fuel rod used in this experiment was fabricated from unirradiated zircaloy-4 cladding and UO_2 fuel. The fuel rod had an active fuel stack length of 0.914 m and was pressurized to 2.58 MPa with a mixture of helium and argon gas (77.7% He and 22.3% Ar) to simulate an end-of-life gas conductivity typical of a commercial PWR fuel rod.

The film boiling test phase was preceded by 16 h of nuclear operation, which included power calibration and preconditioning periods at test rod peak powers up to 57 kW/m. Film boiling was induced by rapidly increasing the test rod peak power from 39 to 69 kW/m at constant coolant conditions (1110 kg/s·m^2 mass flux and 605 K inlet temperature). The test rod power was subsequently adjusted to 77.8 kW/m for the duration of the film boiling test phase. The rod was operated in film boiling for a total time of 900 s, with nominal coolant conditions of 15.2 MPa system pressure, 605 K inlet temperature, and 1050 kg/s·m^2 shroud coolant mass flux. Rod failure occurred 520 s after the start of the power ramp to 69 kW/m (500 s after the first indication of film boiling) due to cladding embrittlement and, as a result, the bottom rod segment dropped 2.7 mm in the shroud. No energetic reactions as a result of the failure or subsequent rod breakup were observed. Cladding collapse onto the fuel stack resulted in greatly restricted fill gas communication between the failure location and other parts of the fuel rod. The fuel rod failure did not significantly degrade the coolability of the rod during film boiling operation, even though some disintegration of the cladding occurred. Shutdown of the reactor and ensuing quench of the rod resulted in additional rod breakup and an 80% reduction in the shroud coolant flow rate.

The FPDS instrumentation indicated a rapid increase in both gamma and delayed neutron activity in the coolant following rod failure, and again following reactor scram. Figure 4 shows the response of these gross detectors during the test. Initial rod failure occurred at 520 s, but transport of the released fission products to the detector station delayed indication for 120 s. Both detectors indicated rod failure with a sharp signal increase of more than two orders of magnitude. Following reactor scram, the signals again increased another order of magnitude as a result of the significant fuel fracturing that occurred upon quench. As expected, the delayed neutron signal decreased rapidly after scram, since the longest lived delayed neutron precursor has a 55-s

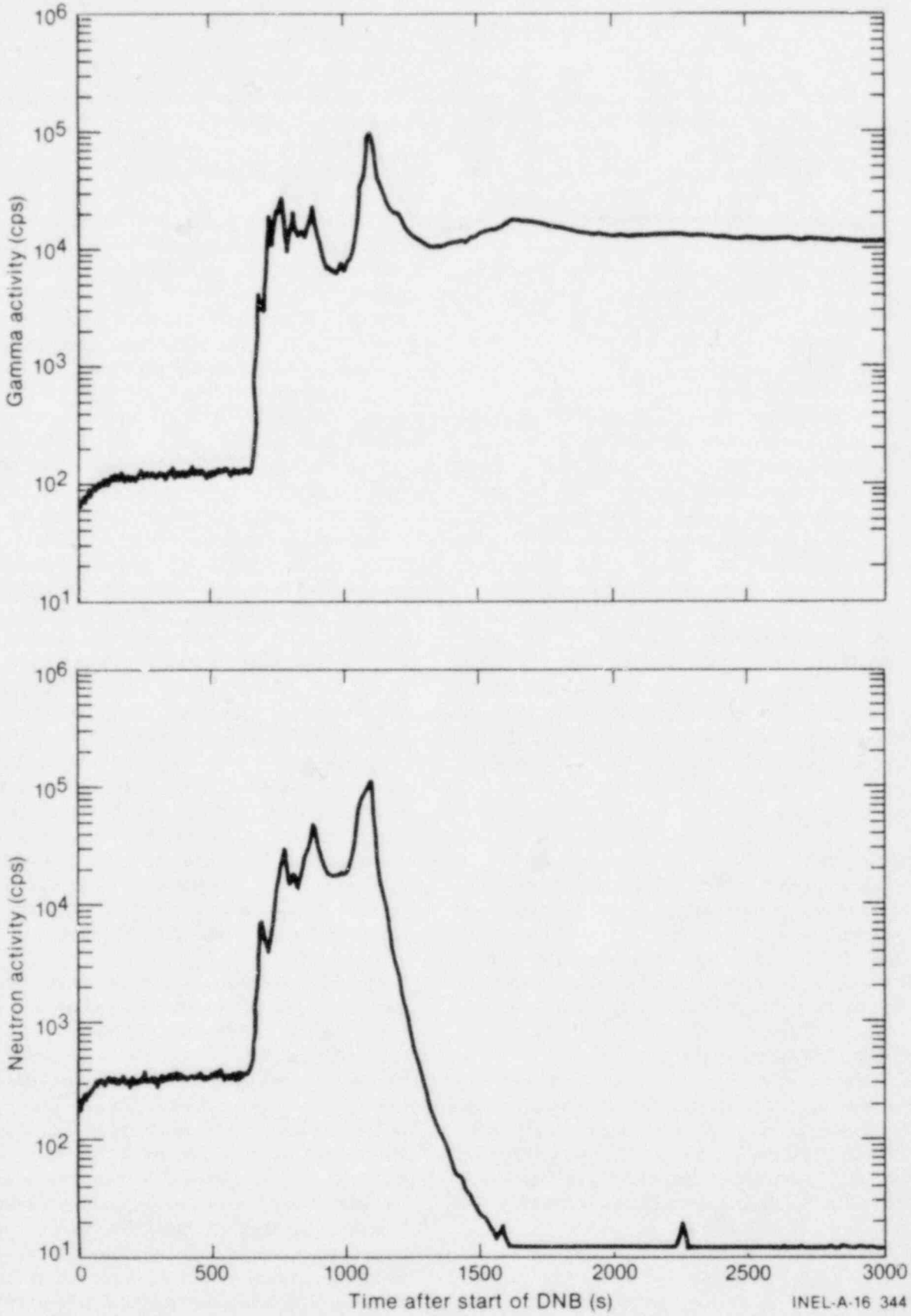

Figure 4. Gross gamma and delayed neutron response during Test PCM-1.

half-life. The gross gamma signal remained high for several hours after scram, permitting detailed gamma spectral measurements. Gamma spectra were acquired in 1-min intervals for ~40 min following rod failure, then in increasing time intervals for an additional 300 min. A coolant sample was also collected after the temperature and pressure of the loop were reduced to near ambient conditions.

The fuel rod was examined after Test PCM-1 to identify and document the overall posttest condition of the rod. The flow shroud was split longitudinally and opened to expose the rod. The split shroud with the failed rod and a scale, indicating distances from the bottom of the shroud, are shown in Figure 5. The lower film boiling boundary is located at 0.35 m on the scale (0.21 m from the bottom of the fuel stack), as indicated by the change from a dark to a light oxide. A major break in the rod occurred at 0.44 m (0.30 m from the bottom of the fuel stack). Above this location are six loose fuel pieces without cladding, one of which is almost two pellet lengths long. Two pieces with cladding partially intact, and a 0.06-m section with the entire cladding intact are located above the fuel pieces. The fuel rod-to-shroud spacing does not permit the interchange of fuel rod pieces, and although some axial movement of the pieces may have taken place, they are assumed to be at their operating locations within the flow shroud.

The top intact portion of the rod begins at 0.80 m (0.63 m from the bottom of the fuel stack), and is positioned in its original axial location in the shroud (the rod was rigidly fixed at the top end cap). The bottom section of rod dropped 2.7 mm in the shroud. Cladding collapse at the pellet interfaces occurred from 0.80 to 0.96 m (0.63 to 0.79 m from the bottom of the fuel stack). The upper film boiling boundary is at approximately 1.02 m (0.85 m from the bottom of the fuel stack).

Evidence of molten fuel extending to 85% of the local pellet radius was found in one fuel specimen. The total fraction of the rod that showed evidence of melting was estimated to be 25%. The estimated maximum cladding temperature was above 2100 K and the maximum fuel temperature reached 3100 K. Twenty-four percent (153 g) of the original fuel stack fragmented or powdered into pieces smaller than 76 μm and was washed out of the flow shroud by the coolant. However, cladding specimens that had been completely oxidized, and cladding sections that had been previously molten (inside a shell of oxide) remained intact following quench and posttest handling.

3.2 RIA Tests

This section describes the Reactivity Initiated Accident Scoping Tests[19] (RIA-ST) conducted in the PBF, three of which included fuel rod failures and provided information about fission product release. The RIA Scoping Tests were enabling tests performed prior to the RIA Test Series. The main objectives of the scoping tests were to evaluate proposed methods for measuring fuel rod energy deposition during a power burst, determine the peak fuel enthalpy threshold for failure, determine the rod failure mechanism of unirradiated fuel rods at BWR hot-startup coolant conditions, and test the response of the PBF reactor system to an extreme energy burst.

The RIA Scoping Tests consisted of four separate, single-rod tests designated RIA-ST-1, RIA-ST-2, RIA-ST-3, and RIA-ST-4. Each test was performed with one unirradiated, zircaloy-clad fuel rod with a 0.914-m active length. Each rod was enclosed in a cylindrical flow shroud sized to provide a coolant flow volume approximately equivalent to the volume per rod in a commercial BWR rod bundle.

The RIA-ST series included two power bursts during RIA-ST-1 and one burst each during RIA-ST-2, RIA-ST-3, and RIA-ST-4. The coolant conditions for each transient were nominally 538 K, 6.45 MPa, and 0.085 L/s, which are representative of BWR hot-startup conditions. Fuel rod failure and fission product release to the coolant loop occurred during the second burst of the RIA-ST-1 experiment, and during the RIA-ST-2 and RIA-ST-4 experiments. A brief discussion of the results of each of these three tests is given below. Since rod failure did not occur during RIA-ST-3, fission products were not released.

3.2.1 RIA-ST-1. Fuel rod conditioning was performed during RIA-ST-1 to promote cracking and relocation of the fuel pellets and to build up a long-lived fission product inventory. An axial peak, radial average fuel enthalpy of 185 cal/g (205 cal/g peak fuel enthalpy near the pellet surface) was achieved in the first power burst of RIA-ST-1. This axial peak, radial average fuel enthalpy

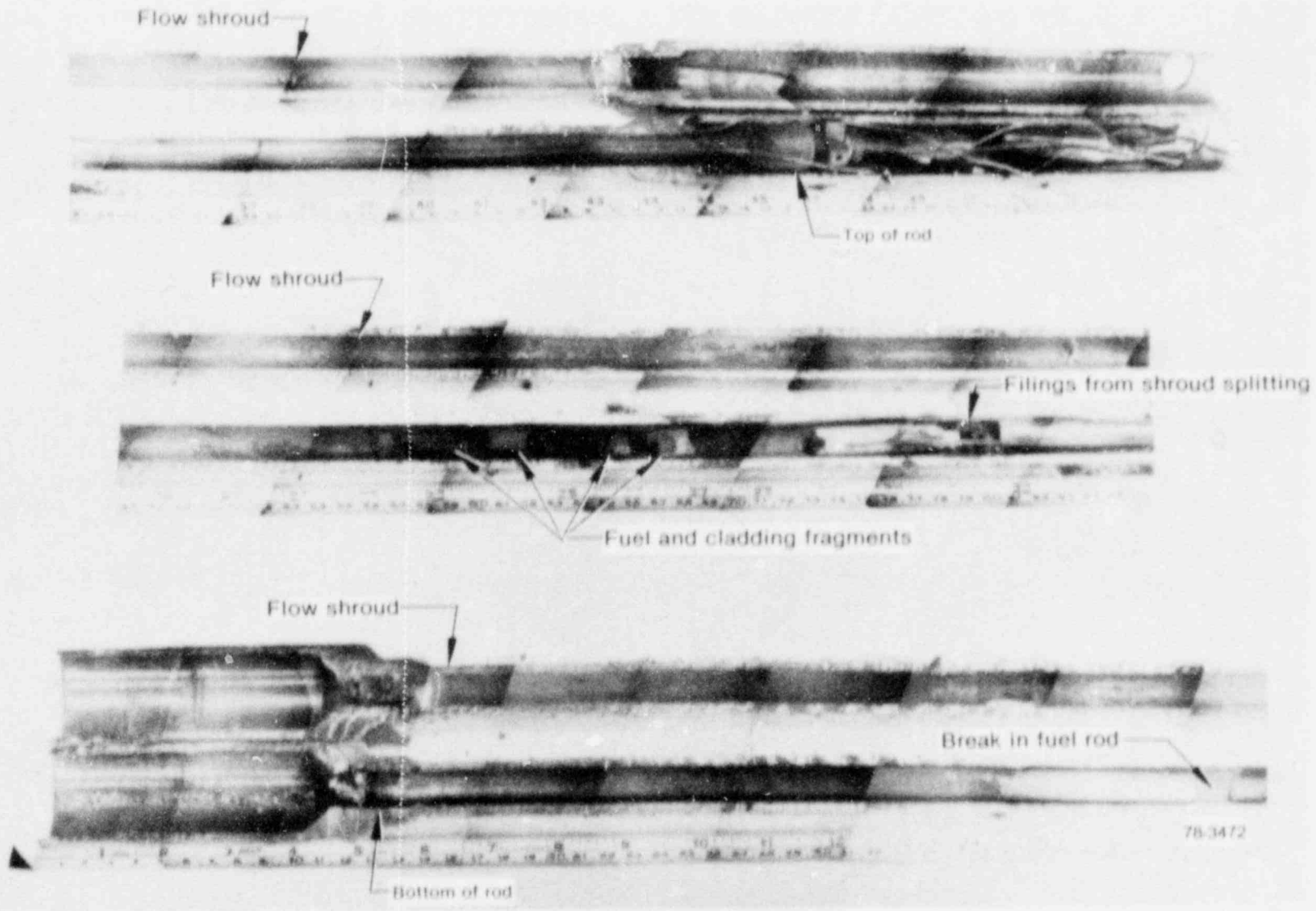

Figure 5. Overall view of Test PCM-1 fuel rod in shroud.

corresponds to a total radial average energy deposition of 250 cal/g UO_2. No indication of fuel rod failure was observed. The second power burst of RIA-ST-1 resulted in an axial peak, radial average fuel enthalpy of 250 cal/g (275 cal/g peak fuel enthalpy), corresponding to a total radial average energy deposition of 330 cal/g UO_2. The FPDS indicated rod failure following this second power burst.

Figure 6 shows the response of the FPDS gross gamma detector. The signal spike at t = 0 corresponds to the prompt fission gamma radiation emanating from the PBF reactor during the power burst. Although the FPDS detectors are well shielded, a small fraction of the intense burst radiation penetrates the shielding and induces a convenient burst time mark on the indicated signal. As a result of the low loop coolant flow rate, the flow rate in the FPDS sample line was also relatively low, resulting in a transport time of 420 s for the fission product release. The gross gamma signal rose sharply upon arrival of the first fission products to the detector station. No delayed neutron signal was observed. The delay time of 420 s is nearly 8 half-lives of the longest lived delayed neutron precursor, which results in nearly complete decay of these fission products before arrival at the detector station. A significant concentration of gamma emitting fission products remained in the coolant for several hours following the test, which allowed monitoring with the gamma spectrometer to identify the dominant isotopes present and their temporal behavior in the loop.

Postirradiation examination of the fuel rod revealed extensive cladding reaction and deformation, including oxide spalling and cladding collapse, fracture, and crumbling. Figure 7 shows the posttest appearance of the RIA-ST-1 fuel rod. The intact portions of the failed rod revealed that cladding oxidation occurred over 95% of the fuel stack length, indicating that film boiling extended over essentially the entire rod length. The rod failed in the high power region during or after cladding quench. As evident in Figure 7, the cladding experienced massive oxidation, oxide spalling, splitting and fracture, and ridging. Approximately 10% of the fuel from the highly damaged region was discharged to the coolant stream and washed out of the test train. This fine particulate fuel contributes to the fission product release measured by the FPDS.

Figure 8 shows the calculated time-dependent temperature responses of a fuel rod exposed to a power burst resulting in an axial peak, radial average fuel enthalpy of 260 cal/g. Partial melting of the fuel and cladding was predicted to occur.

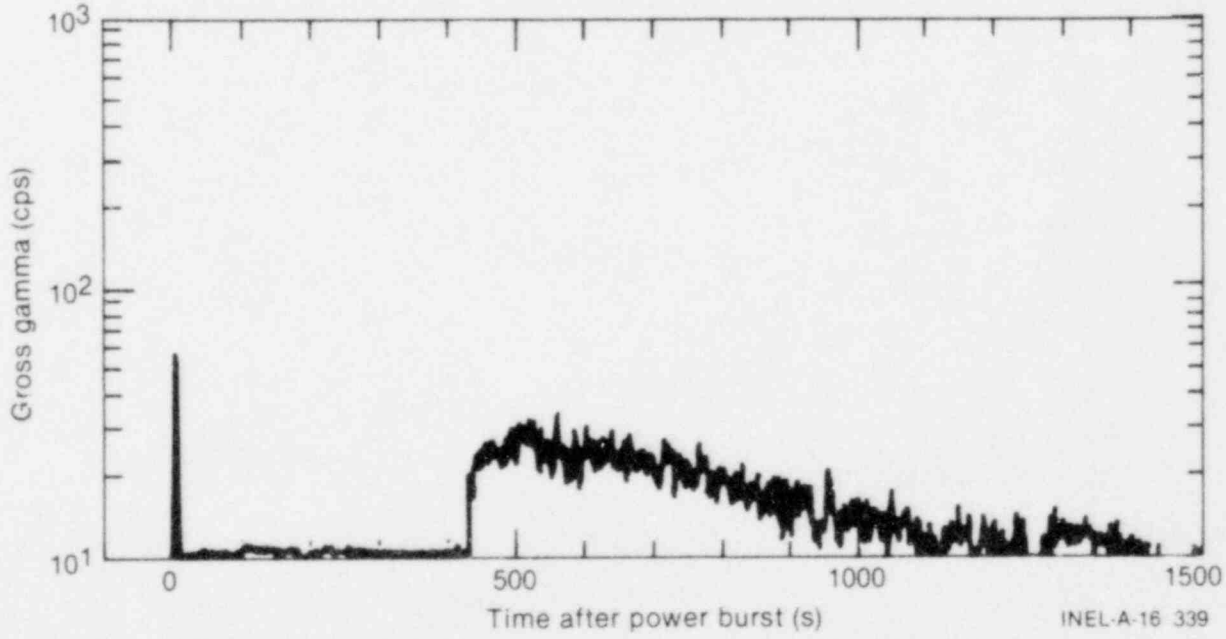

Figure 6. Gross gamma response during RIA-ST-1.

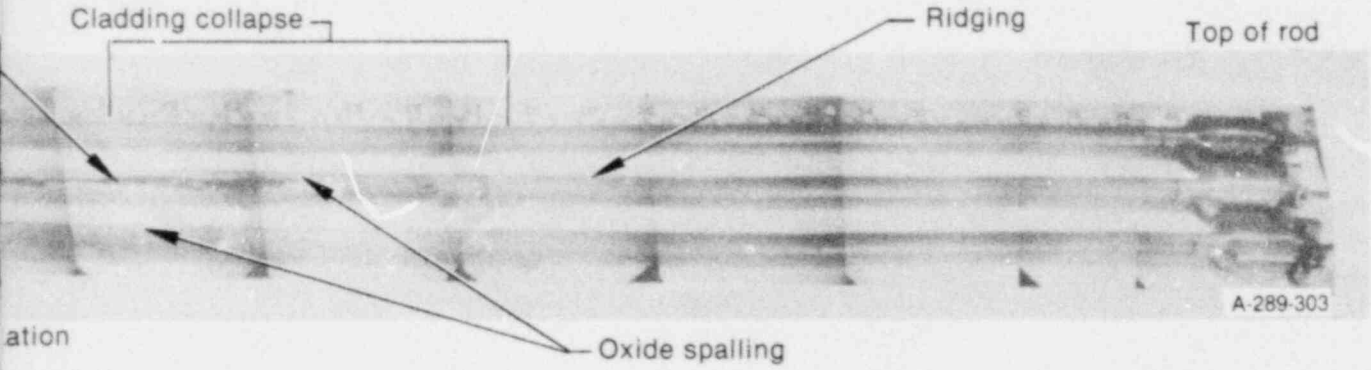

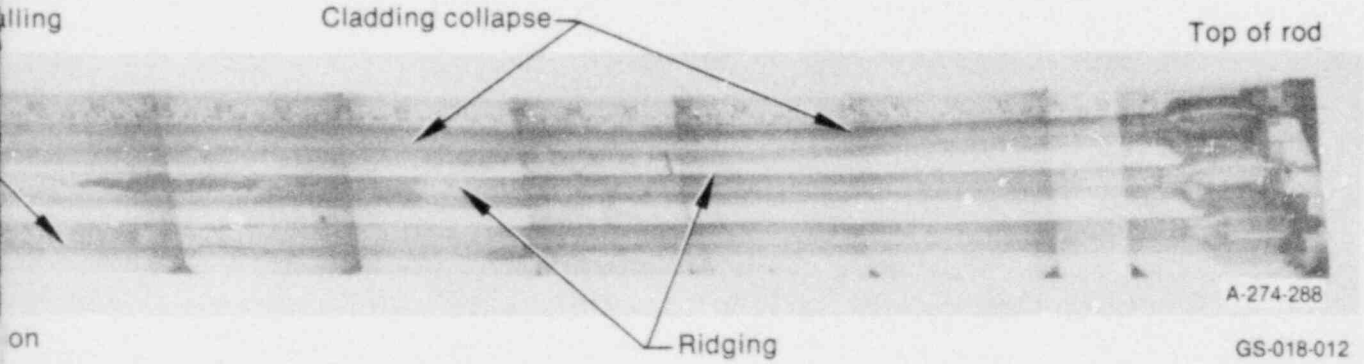

m RIA-ST-1, RIA-ST-2, and RIA-ST-3.

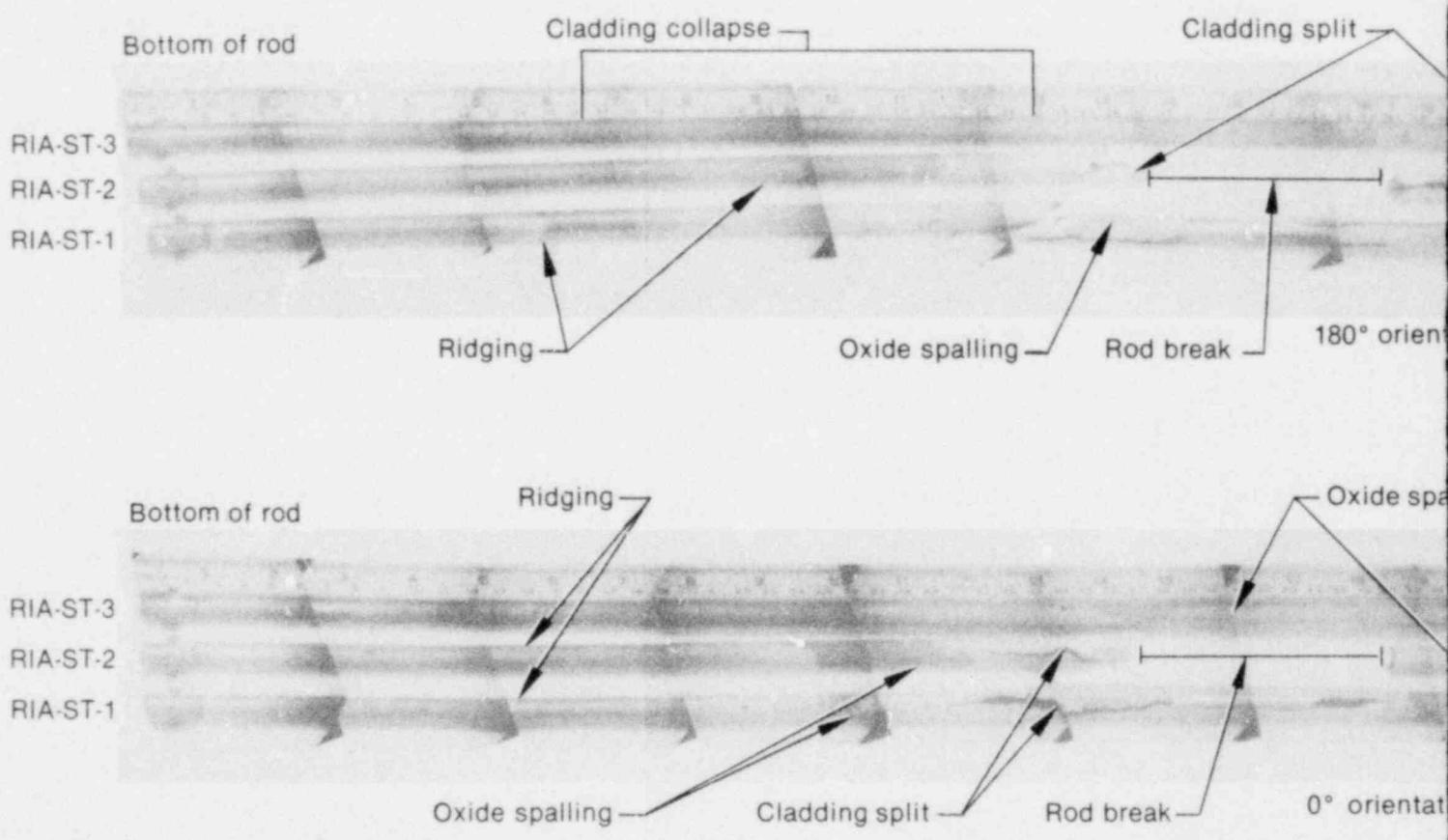

Figure 7. Posttest photograph of fuel rods fro

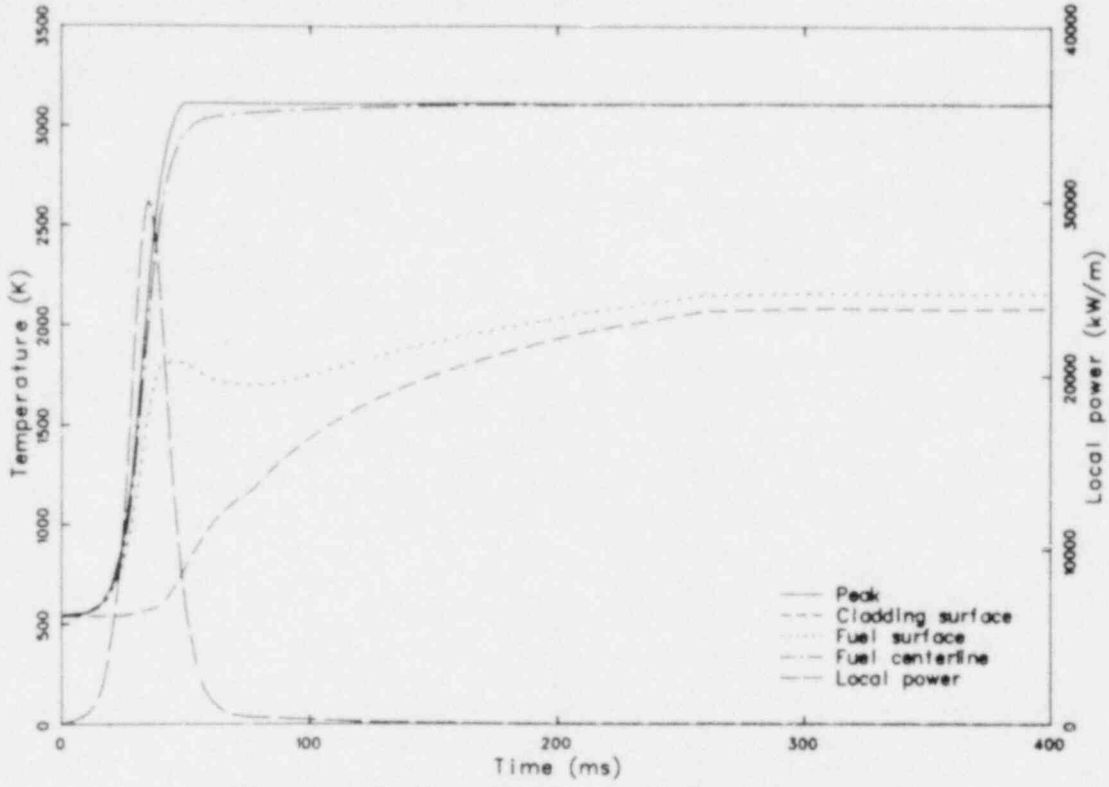

(a) 400-ms time scale showing temperature transients during the power burst

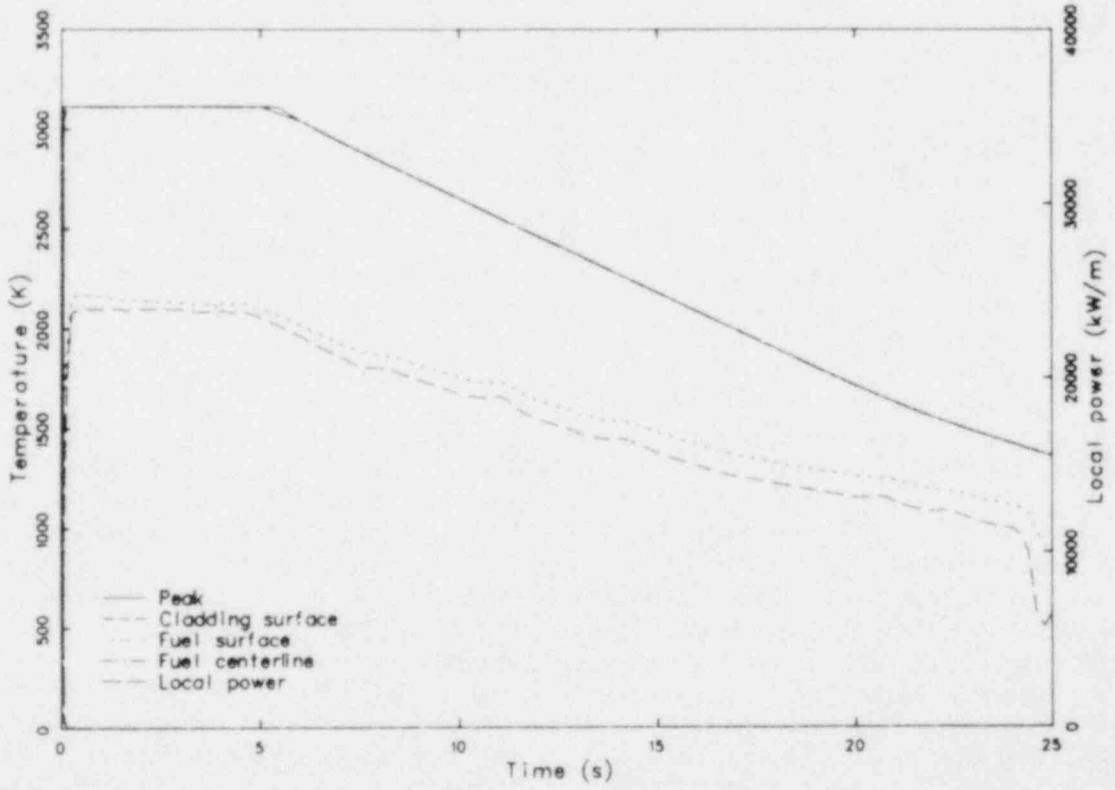

(b) 25-s time scale showing temperature transients over the full dryout range

Figure 8. Calculated fuel rod temperature histories for an axial peak, radial average fuel enthalpy of 260 cal/g.

Posttest microstructures showed no evidence of fuel pellet melting or columnar grain growth, although partial melting of the fuel-cladding interaction zone was observed.

Fuel shattering or powdering (UO_2 grain boundary separation) was observed in some specimens. The data indicate that complete fuel powdering occurred for axial peak, radial average fuel enthalpies of >230 cal/g (>255 cal/g axial peak), and that partial shattering occurred for axial peak, radial average fuel enthalpies greater than ~185 cal/g (205 cal/g peak). Although some fracturing of the fuel was expected to occur during preconditioning and during the power burst, most of the granular powdering was caused by the rapid cooling as the rod quenched.

3.2.2 RIA-ST-2. The RIA-ST-2 fuel rod was exposed to a single power burst, with no significant steady state operation. The axial peak, radial average fuel enthalpy achieved from this single power burst, 260 cal/g (peak fuel enthalpy of 290 cal/g and total radial average energy deposition of 345 cal/g UO_2), resulted in rod failure.

The gross gamma detector response during RIA-ST-2 was very similar to that during RIA-ST-1, which is shown in Figure 6. The power burst was indicated at t = 0, and a sharp rise in the signal occurred after a 450-s delay time. The magnitude of the RIA-ST-2 signal was slightly higher. Although the RIA-ST-1 rod received a greater irradiation as a result of the power calibration phase and extra power burst, there was a delay of more than three days before the second RIA-ST-1 power burst, allowing significant decay of the important short-lived fission products. Thus, the principal short-lived fission product inventory released during both tests was generated during the power bursts, which differed in radial average peak fuel enthalpies by ~5%.

Figure 7 also shows the posttest appearance of the RIA-ST-2 rod, which is similar to that of the RIA-ST-1 rod. Massive oxidation, oxide spalling, cladding splitting and fracture, and cladding ridging occurred. Approximately 15% of the fuel was lost to the coolant loop. The detailed metallographic examination of both the RIA-ST-1 and RIA-ST-2 rods showed similar results; no evidence of fuel melting or grain growth was observed.

3.2.3 RIA-ST-4. The RIA ST-4 fuel rod was irradiated during a power calibration phase, which was completed 38 h prior to the power burst. Thus, the principal short-lived fission product inventory released during the test was generated during the burst. The axial peak, radial average fuel enthalpy resulting from the RIA-ST-4 power burst was 350 cal/g (peak fuel enthalpy of 530 cal/g and total radial average energy deposition of 695 cal/g UO_2) at the time of rod failure. A power transient of this magnitude is greater than is possible in a commercial reactor during an RIA. The purpose of this test was to evaluate the magnitude of potential pressure pulses and the potential for molten fuel-coolant interaction resulting from inadvertent high energy rod failure in the PBF liquid filled test loop. This test also offered an opportunity to monitor fission product release from molten fuel to the pressurized coolant loop. As expected, this large energy deposition resulted in immediate fuel rod failure.

Figure 9 shows the response of the gross gamma and the delayed neutron monitors during RIA-ST-4. The large burst of core radiation can be seen at t = 0 and the sharp rise in both signals at 190 s. (The shorter delay time of 190 s during this test is the result of the higher loop flow rate.)

The high concentrations of fission products measured during this test provided a substantial challenge to the FPDS. Electronic dead time as a result of piled-up pulse rejection reached ~60%; however, the quality of spectral resolution was not significantly degraded and accurate spectral analysis was accomplished without special refinements. Conventional monitoring equipment, which was also used to monitor RIA-ST-4, experienced electronic saturation due to the extremely high gamma source and was unable to collect usable information until the fission product concentration had decayed for several hours.

Severe fuel fragmentation occurred during RIA-ST-4; a total of 155 g of fuel fragments were collected from within the test train. Approximately 90% (570 g) of the fuel melted. Approximately 75% (475 g) of the previously molten fuel was found adhering to the inside surface of the flow shroud (see Figure 10). Fuel lost to the coolant loop was estimated to be <1%. Most of the particles found in the test train were spherical or rounded, suggesting the fuel was molten at the time it fragmented. A maximum RIA-ST-4 fuel temperature of about 3740 K was calculated; however, detailed posttest analysis[20] suggests that 3500 K is the probable maximum temperature reached by the UO_2 fuel.

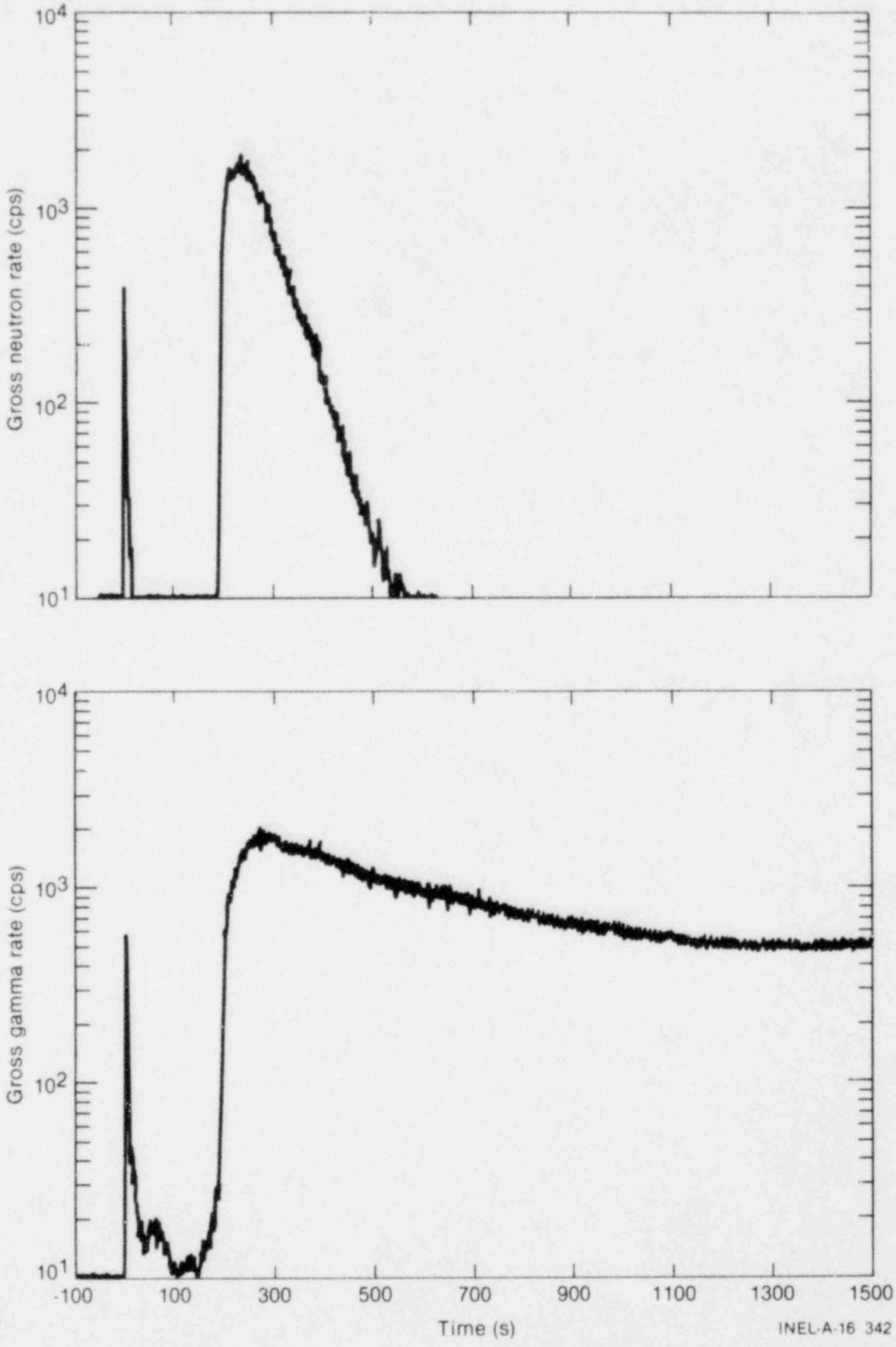

Figure 9. Gross gamma and delayed neutron response during RIA-ST-4.

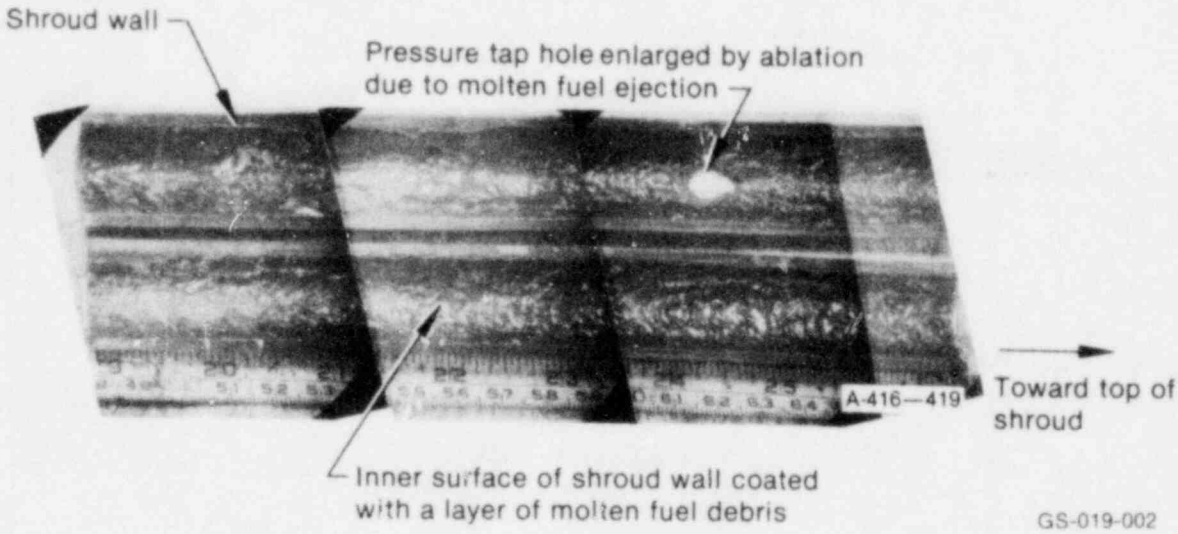

Figure 10. Posttest photograph of RIA-ST-4 fuel found adhered to the inside surface of the flow shroud.

4. FISSION PRODUCT BEHAVIOR

The release of radioactive fission products from a nuclear power plant poses a radiological hazard that is of major concern to the NRC and the nuclear industry. For this reason, accurate description of fission product behavior during normal and accident situations is recognized as a very important aspect of reactor safety. This understanding could provide the means for a more realistic description of accident source terms, and could also enhance the ability to ascertain the fuel conditions that prevail in a reactor core during normal operation or following an accident. The prime objective of the PBF fission product studies is to experimentally investigate fission product behavior. This section discusses the important factors affecting fission product behavior, presents the results of the fission product release measurements, examines the PBF results for insights into the relationships between fuel behavior and fission product release, and compares the test results with fission product release fractions found in NRC Regulatory Guides, the Reactor Safety Study, and the Three Mile Island accident data.

4.1 Reporting Release Fractions

The behavior of fission products is very complex. It is not presently possible to accurately describe, either analytically or empirically, the behavior of this complex system. It is possible, however, to monitor and document some of this behavior, and to relate the measurements to the important controlling parameters.

The fact that the fission products are radioactive permits detection and quantification of minute quantities, but this also complicates their behavior. All radioactive fission products are born as members of one of several decay chains. The usual form of decay is by emission of a beta particle coincident with the identifying gamma ray. As illustrated in Figure 11, this beta decay produces a change in the atomic number of the isotope and, thus, an elemental change in the fission product. The chemical and physical nature of the daughter fission product will be different than that of the parent. The chalcogens decay to halogens, which in turn decay to a noble gas isotope. Beta decay of a noble gas isotope will produce an alkali metal, and further decays will follow through to alkaline earth and rare earth isotopes. The physical behavior is further complicated by the different half-lives, fission yields, and branching ratios of the different isotopes. Chemical behavior will be influenced by the presence of varying concentrations of stable fission products.

During tests in the PBF, as with operation in nuclear power plants, the irradiation histories fluctuate, preventing establishment of equilibrium

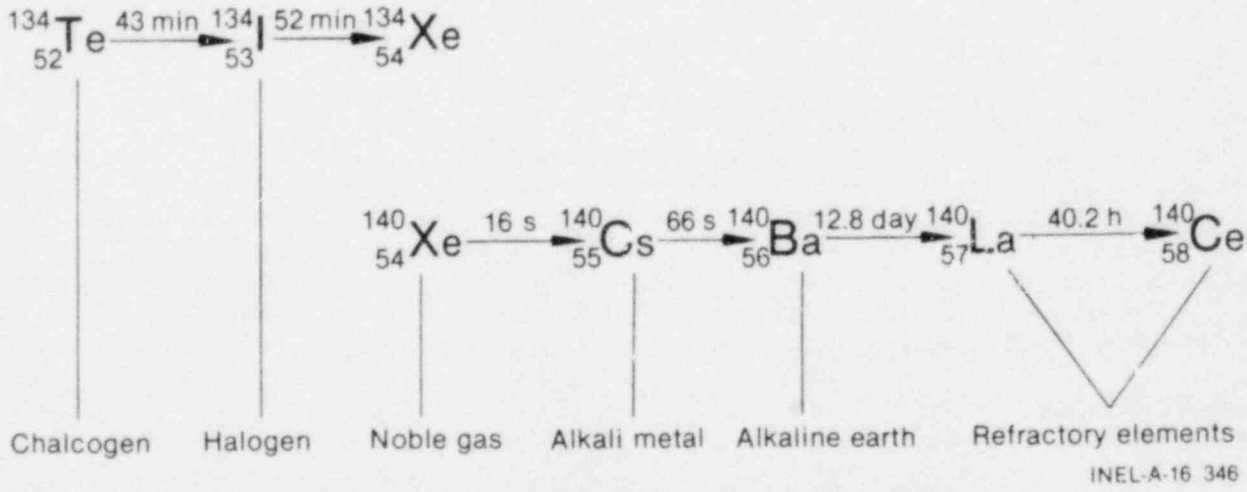

Figure 11. Schematic diagram of typical fission product decay chains.

fission product inventories. The measurement and interpretation of fission product data from circulating coolant loops with varying temperature, pressure, and flow rate are difficult. In spite of the complexities, some helpful information about fission product behavior can be derived from the PBF tests by comparing key fuel behavior parameters to the measured isotopic release fractions.

A useful technique employed by most investigators to aid in understanding fission product behavior is to measure isotopic release fractions (RF). During steady state operation, release-to-birth ratios are descriptive of the amounts of fission products leaving the fuel or fuel rod. During accidents, the release-to-total inventory ratio is more descriptive, because during such transients the isotopic birth rate is fluctuating or zero as a result of power changes or reactor scram.

Early in the test program, it was realized that the release fractions alone are not sufficiently descriptive of the fission product source terms. The measured coolant release fractions are actually time dependent due to the duration of the releases and the behavior of the fission products in the coolant loop. Knowledge of the time-dependent release fractions is useful in accident analysis for estimating source terms to the containment building atmosphere. If the source term challenging the containment atmosphere cleanup systems is to be realistically evaluated, the time required for release must be incorporated into the analysis. If a particular fission product, such as iodine, is reacting in the coolant loop such that it is deposited or otherwise unavailable for transport, this reduction in the inventory fraction must be considered in calculating the time-dependent source term to containment. The release fraction histories are, therefore, a more descriptive format than a single-valued release fraction. The fission product release information reported here for the PBF tests is in the format of release fraction histories RF(t). The complete set of 69 isotopic release fraction histories is given in Appendix A with a description of the methodology used in generating them.

4.2 Release Fraction Calculation

When a fuel rod failure occurs and fission products present in the fuel-cladding gap are released to the coolant, a burst or spike of fission product activity will pass by the radiation monitors and then proceed through the loop, becoming more thoroughly mixed. Figure 12 shows the measured concentration history for ^{88}Rb during Test PCM-1 and serves to illustrate the typical behavior. The initial high concentration measured during the spike is not indicative of the fission product concentration throughout the entire loop, but it is indicative of the relative magnitude and timing of the release. Following the spike release is a longer lived, secondary or leaching release of fission products associated with the exposed fuel and cladding internal surfaces. This release may persist for hours following rod failure, but eventually reaches a minute level at which it becomes indistinguishable in the presence of the fission product concentration in the loop. The total quantity of fission product released, R(t), can be calculated by multiplying the fission product concentration in the coolant, C(t), by the loop volume, V

$$R(t) = C(t) \times V.$$

Measurement of the time-dependent concentration allows the time-dependent release quantity to be calculated. The release fraction history, RF(t), can then be determined by dividing the quantity released, R(t), by the total inventory, I(t)

$$RF(t) = \frac{C(t) \times V}{I(t)}.$$

The result of performing this conversion on the ^{88}Rb example is illustrated in Figure 13.

This technique requires multiplication of the entire loop coolant volume by the local fission product concentration measured at the detector station. During the early period following rod failure, before sufficient mixing of the fission product occurs, this calculation may result in instantaneous release fractions exceeding 100%. Although this result is not strictly valid and can be somewhat misleading, it permits the description of the fission product release pattern and a qualitative interpretation of the temporal behavior of the release. The calculated release quantities, and therefore the release fractions, are not strictly valid until the fission products are reasonably well mixed. It is presently estimated that the fission products become well distributed within 8 to 15 min following release from the fuel rod.

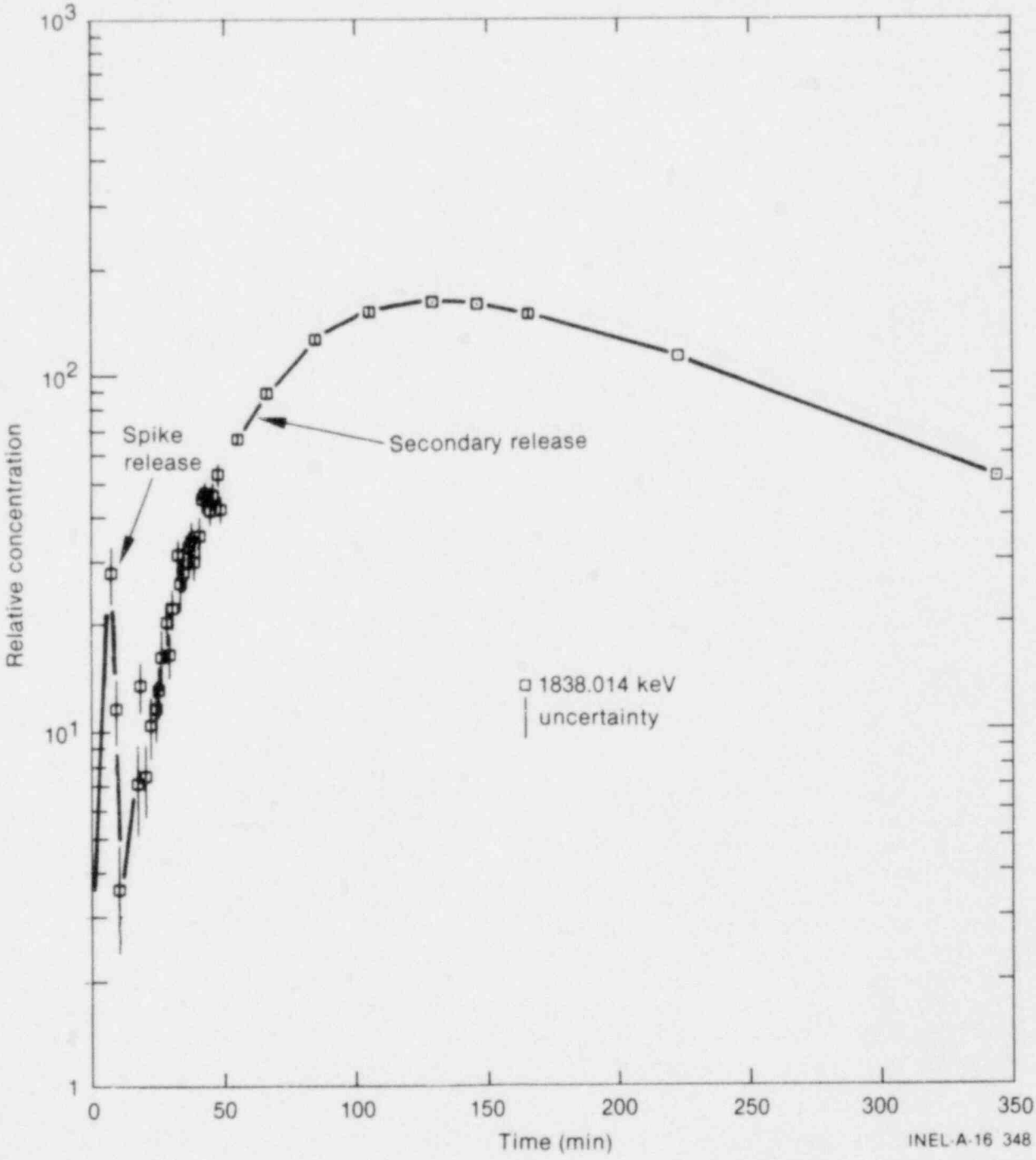

Figure 12. Concentration history of ^{88}Rb during Test PCM-1.

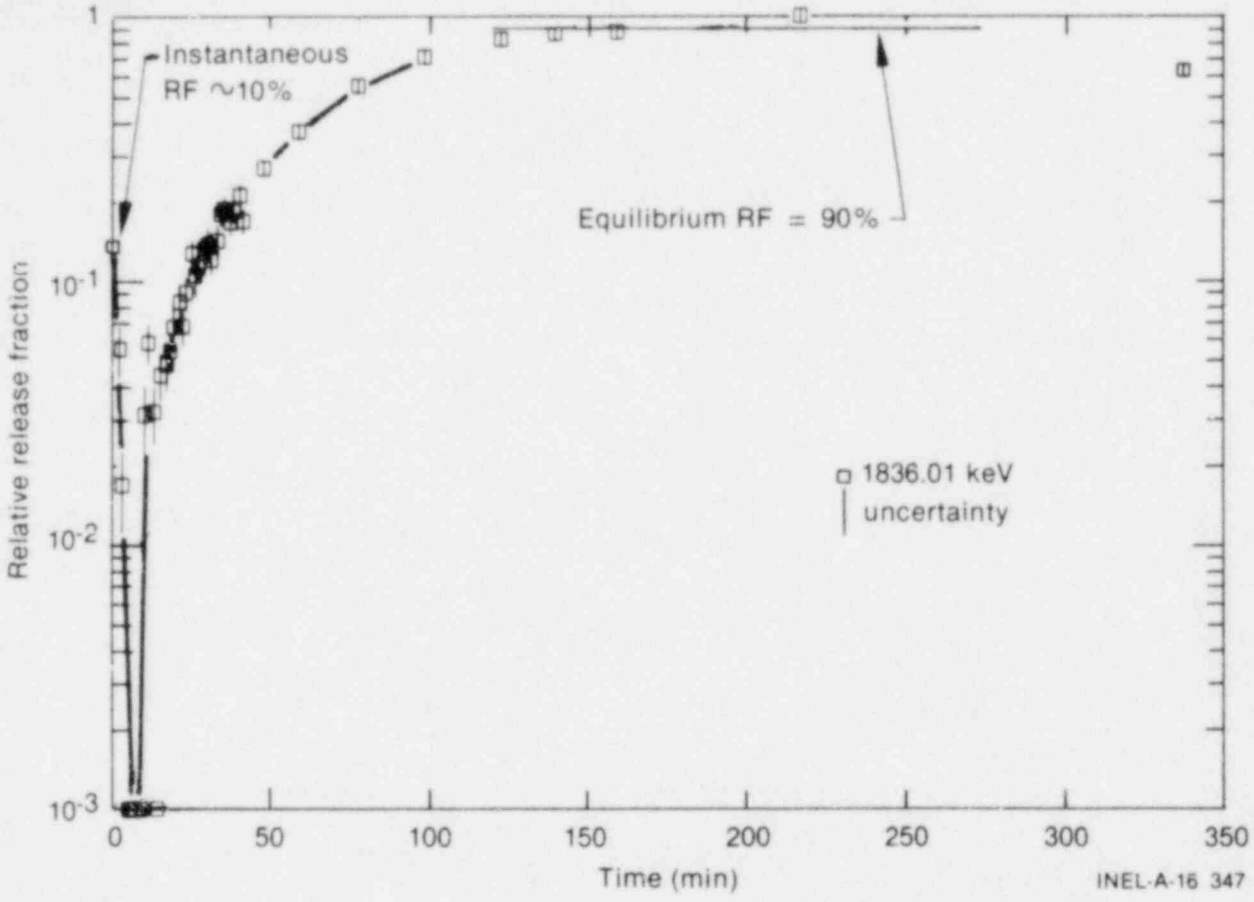

Figure 13. Release fraction history of ^{88}Rb during Test PCM-1.

The advantages of reporting the data in this format are realized when comparing release patterns for different isotopes and for different tests. Larger burst release fractions indicate that greater percentages of the fission products are released during initial rod failure. Larger secondary release fractions indicate that greater percentages of the fission products are released during the extended time period following rupture. A gradual rise in the release fraction history indicates a long-lived source term, but an early rise to a stable release fraction value indicates a short-lived source term.

In addition to the two-phase (spike plus secondary) release, the possibility exists for another source term resulting from the radioactive decay of the parent isotope present in the coolant. The analytical discription of the isotopic concentration history must include all of these sources (release from the rod plus parent decay in the coolant), as well as the appropriate loss terms. Loss of the fission products from the coolant will result from radiocative decay and removal processes. Although no cleanup device was employed in the PBF loop during the tests, some removal occurs as a result of processes such as particle settling, chemical reactions, plateout or deposition, etc. Assuming that mixing was instantaneous and that the removal processes can all be lumped together as a single, first-order effect, the concentration rate equation describing the time-dependent concentration of a nuclide, $C_m(t)$, becomes

$$C_m(t) = \frac{dN_m}{dt} = R_m(t) + N_{m-1}\lambda_{m-1} - N_m\lambda_m - \ell_m N_m$$

where

N_m = number of atoms of nuclide m in the coolant

$R_m(t)$ = time varying release of nuclide m from the failed rod

N_{m-1} = number of atoms of nuclide m-1 (parent of m) in coolant

λ_{m-1} = decay constant of nuclide m-1

λ_m = decay constant of nuclide m

ℓ_m = loss coefficient of nuclide m due to particle settling, plateout, and reactions that remove the nuclide from the coolant.

This rate equation is coupled to the rate equation for the parent nuclide N_{m-1}, and also to any grandparent rate equations that may be required. When release from the failed rod subsides and parent concentrations decay to insignificant levels, the source terms disappear and the rate equation becomes

$$\frac{dN_m}{dt} = -N_m \lambda_m - \ell_m N_m \qquad t > t_e$$

$$= -(\lambda_m + \ell_m) N_m$$

$$= -\lambda_{eff} N_m$$

and the behavior of nuclide m can be described by

$$N_m(t) = N_m^o e^{-\lambda_{eff}(t - t_e)}$$

where

N_m^o = the concentration of nuclide m at time t_e

t_e = time when sources (including parent decay) have ceased

$\lambda_{eff} = \lambda_m + \ell_m$ = effective decay constant.

The interesting feature of this equilibrium behavior is that it offers the opportunity to measure λ_{eff} and thus calculate the loss coefficient $\ell_m = \lambda_{eff} - \lambda_m$. The magnitude of ℓ_m will also be important in determining the equilibrium release fraction, since significant losses will produce a constant decline in the observed RF(t). This may be important for estimating release from the primary system to containment, especially for instances in which ℓ_m is temperature- or pressure-dependent and the accident scenario includes depressurization and temperature fluctuations.

This phenomenon also permits some additional interpretation of the PBF data, even though the loss coefficients may be unique to the PBF coolant loop. The rate of decrease of the equilibrium release fraction value indicates the rate of removal of the fission product from the coolant, and a steady release fraction value indicates that no removal processes are affecting the isotope in the coolant loop. Of course, there is also the possibility of balancing a slow, long-lived source term by an equal long-lived removal term. This condition results in a constant value of the isotope concentration in the coolant for estimates of the release to containment.

4.3 Equilibrium Release Fractions

The results of the fission product behavior measurements taken during the four PBF tests are presented in this section with a brief discussion of the outstanding features. A summary of the important fuel behavior parameters from each test is given in Table 1, and a summary of the measured fission product release fractions for each test is given in Table 2. The summary format is a listing of the normalized isotopic release fractions of the principal fission products measured after the isotopes reached equilibrium concentration. Because the FPDS was still in its developmental stages when these data were collected, the absolute calibration of the spectrometer was uncertain. Therefore, to provide the most conservative estimate of the fission product release fractions, it was necessary to normalize these data to a value of 1.0 for the largest release fraction measured in each test. This procedure ensures that the numbers presented represent a maximum upper limit of the isotopic releases experienced by the UO_2 fuel in each test. The normalization was applied uniformly to each release fraction in a specific test to generate relative magnitudes for isotope release fractions. Although this technique prevents direct comparison of absolute release fractions between different tests, it does allow for useful interpretations through comparisons of various ratios of relative release fractions from one test to another.

It should be emphasized that for realistic accident analysis, the entire time-dependent release fractions should be considered. For convenience, only the best estimate of the equilibrium release

Table 1. A comparison of fuel behavior parameters during the PBF tests

	PCM-1	RIA-ST-1	RIA-ST-2	RIA-ST-4
Transient condition[a]	900 s in film boiling	250 cal/g UO_2 burst	260 cal/g UO_2 burst	350 cal/g UO_2 burst
Number of fissions[b]	1.4×10^{19}	2.6×10^{16}	2.7×10^{16}	4.7×10^{16}
Fuel melted (%)	25	0	0	>90
Fuel lost to loop (%)	24	10	15	<1
Maximum fuel temperature (K)	3100	3000	3000	3500

a. RIA burst values are radial average fuel enthalpy at the axial flux peak.

b. These numbers represent the approximate number of fissions associated with the short-lived fission products, that is, the number of fissions produced in the final departure from nucleate boiling phase of Test PCM-1 and the final power burst in each RIA test.

fraction values are summarized in Table 2. The entire time-dependent release fraction, RF(t), requires two-dimensional representation. These release fraction histories are included in Appendix A with a description of the methodology used in generating the plots.

Fission product behavior during PBF tests is generally characterized by large noble gas release fractions, medium to high rubidium release fractions, low to medium iodine release fractions, and widely varying cesium, barium, and lanthanum release fractions. Whereas a noble gas isotope demonstrated the largest release in Tests PCM-1 and RIA-ST-2, ^{142}La exhibits the largest release in RIA-ST-1 and RIA-ST-4.

An outstanding feature of these data is the large differences in release fractions of the radiologically important iodine isotopes. As illustrated in Figure 14, the iodine release fractions were very small compared to the noble gas release fractions in the two tests that produced high fuel temperatures and large percentages of fuel melting (Tests PCM-1 and RIA ST-4). The other two tests (RIA ST-1 and RIA ST-2), which produced no evidence of fuel melting, show larger fractions of iodine release relative to the noble gas releases. The iodine may be vaporized and driven out of the fuel at these high temperatures (3100 to 3500 K), but the results suggest that the iodine quickly deposits on the cladding or test train materials to bind the isotope and prevent transport in the coolant. During the lower temperature tests (< 3100 K) the iodine may be sufficiently volatilized to be driven out of the fuel, but the cladding or coolant conditions may be substantially different, possibly preventing early deposition.

Another surprising result is the large difference in release fractions among different isotopes of the same element. Both ^{140}Ba and ^{140}La show substantially lower release fractions than the ^{142}Ba and ^{142}La during the three RIA tests. Barium is considered to be a member of the low volatility group of fission products, and lanthanum is a member of the refractory group, yet the release fractions observed during the RIA tests for ^{142}Ba-La are large and those for ^{140}Ba-La are much lower. The release fractions for Ba and La during Test PCM-1 were very low, as would be expected for elements in these low volatility or refractory groups.

Table 2. Normalized fission product release fractions

	Test PCM-1		RIA-ST-1		RIA-ST-2		RIA-ST-4	
Isotope	RF	Uncertainty	RF	Uncertainty	RF	Uncertainty	RF	Uncertainty
^{85}Kr	1.00	0.07	a		a		a	
^{87}Kr	0.92	0.08	0.55	0.15	0.44	0.06	0.26[b]	0.03
^{88}Kr	0.93	0.07	0.49	0.06	0.46	0.08	0.62[b]	0.08
^{88}Rb	0.90	0.07	0.64	0.09	0.63	0.12	0.81[b]	0.10
^{89}Rb	0.020	0.001	0.56	0.11	0.67	0.10	0.18	0.02
^{131}I	a		0.23	0.03	c		0.048	0.009
^{132}I	0.012	0.001	0.23	0.02	c		0.053	0.007
^{133}I	0.017	0.001	0.21	0.02	0.34	0.08	0.042	0.006
^{134}I	0.015	0.001	0.32	0.04	0.36	0.06	0.064	0.008
^{135}I	0.024	0.007	0.62	0.09	c		0.056	0.007
^{135}Xe	0.86	0.05	0.15	0.02	0.30	0.06	0.82[b]	0.10
^{138}Xe	0.86	0.07	0.75	0.11	1.00	0.14	0.85	0.11
^{138}Cs	0.15	0.04	0.43	0.04	0.55	0.08	0.45	0.06
^{139}Cs	0.020	0.004	0.75	0.15	1.3[d]	0.3	0.19	0.02
^{139}Ba[c]	0.0075	0.0013	0.62	0.40	0.87	0.16	0.52	0.07
^{140}Ba	a		0.13	0.02	c		0.021	0.003
^{141}Ba	0.0024[e]	0.0003	0.32	0.04	0.67	0.08	0.40	0.04
^{142}Ba[f]	a		0.31	0.06	0.66	0.10	0.47	0.06
^{140}La	a		0.13	0.02	c		0.021	0.002
^{142}La	0.0019[e]	0.0004	1.00	0.13	0.69	0.08	1.00	0.12
^{143}Ce	a		a		c		0.012	0.003

a. Coolant concentration levels for these nuclides were below detectable levels.

b. During the time interval in which a normalized release fraction was determined, the values of the data points were generally monotonically increasing.

c. Background coolant concentration levels for these nuclides released during RIA-ST-1, seven days earlier, overwhelmed the magnitude of nuclide releases occurring during RIA-ST-2.

d. The normalized release fraction of ^{139}Cs for RIA-ST-2 appears to represent a situation in which uniform mixing was not complete.

e. These values should be interpreted as statistically marginal upper limits, since their presence was observed in only a few spectra.

f. The values shown in this table will disagree with values seen in the relative release fraction plots in Appendix A because of photopeak decontamination.

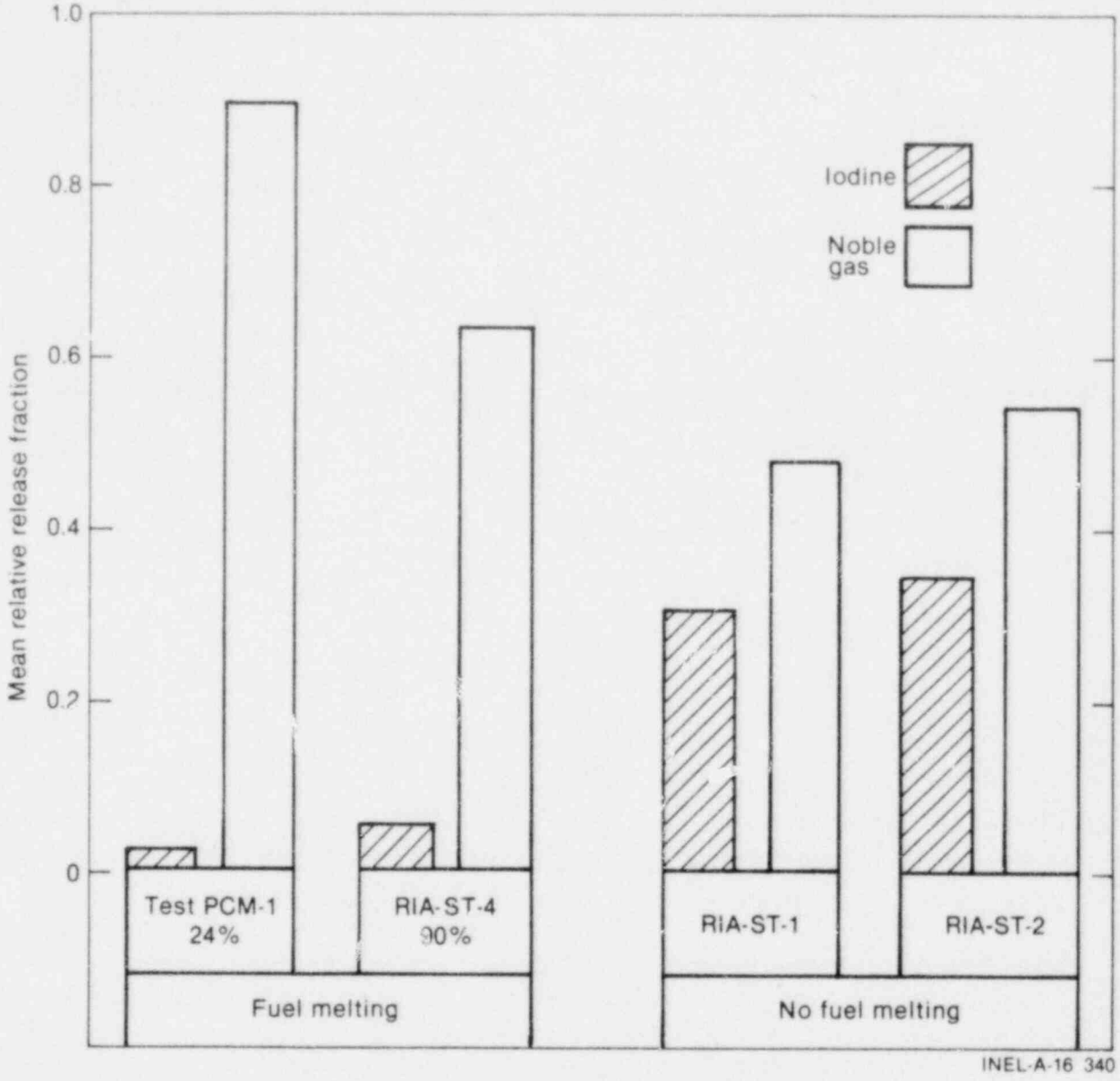

Figure 14. A comparison of the iodine-noble gas release fractions during tests with and without fuel melting.

This fission product "misbehavior" is probably due to the unique circumstances developed in burst-type fuel rod tests. The short periods of irradiation, with associated short temperature transients, create fission product behavior phenomena that also occur over short time periods. Many of the fission product isotopes have short-lived parents and grandparents. The complex chemical and physical changes of the short-lived fission products (as mentioned in Section 4.1) play an important role in the resultant behavior. There are also large differences (a factor of 10^2 to 10^3 in some cases) in the inventories of certain fission products in the different tests, and this could have a marked effect on the measure release fractions.

Another point of interest found in the PBF test results is the demonstration of a significant loss coefficient for iodine during the RIA-ST-1 experiment. As noted in Section 4.2, the rate at which any isotope is removed from the circulating coolant can be estimated from the slope of the release fraction at times after equilibrium has been established. Most of the fission products display a very stable release fraction, with a few exceptions.

The relative release fractions of ^{131}I, ^{132}I, and ^{133}I during RIA-ST-1 reached an equilibrium release fraction of about 25% for the time period up to 300 min following failure. After 300 min, each of the three iodine isotopes begins a dramatic decline to a new level near 3%. The iodine is apparently being selectively removed from the circulating coolant while the other fission products remain unaffected. Figure 15 shows the relative release fraction history of ^{131}I during RIA-ST-1, which is typical of this behavior. Following the second power burst of RIA-ST-1, reduction of the PBF loop coolant temperature and pressure was initiated. The dramatic change in the iodine loss coefficient could be due to the change in the coolant conditions. This behavior serves to illustrate the importance of fission product transport to source term definition. The estimated release fraction could change by an order of magnitude for accidents with different primary coolant conditions.

A phenomenon that displays the opposite effect, a rising release fraction, was observed in the release fraction histories of several isotopes measured during the RIA-ST-4 experiment. The ^{135}Xe release fraction history shown in Figure 16 is an excellent example of a long-lived source term. The positive slope of the release fraction indicates that it has not reached equilibrium. Its parent ^{135}I is still decaying to produce the ^{135}Xe, but the iodine has already been accounted for in the inventory calculation. Therefore, a ^{135}Xe release must still be present, feeding the measured release fraction. This is not surprising, since during RIA-ST-4 the molten fuel coated the inside surface of the coolant shroud, creating a large surface area for fission product transfer from the fuel to the coolant. This apparent source term was seen in several of the other isotope measurements during RIA-ST-4 (see Appendix A), indicating that the phenomenon is not specific to the ^{135}I-Xe decay chain.

4.4 Comparison of Suggested and Reported Release Fractions

The methods used for estimating accident consequences rely on the application of fission product release fractions to the reactor core inventory to predict the amount of radioactive material that

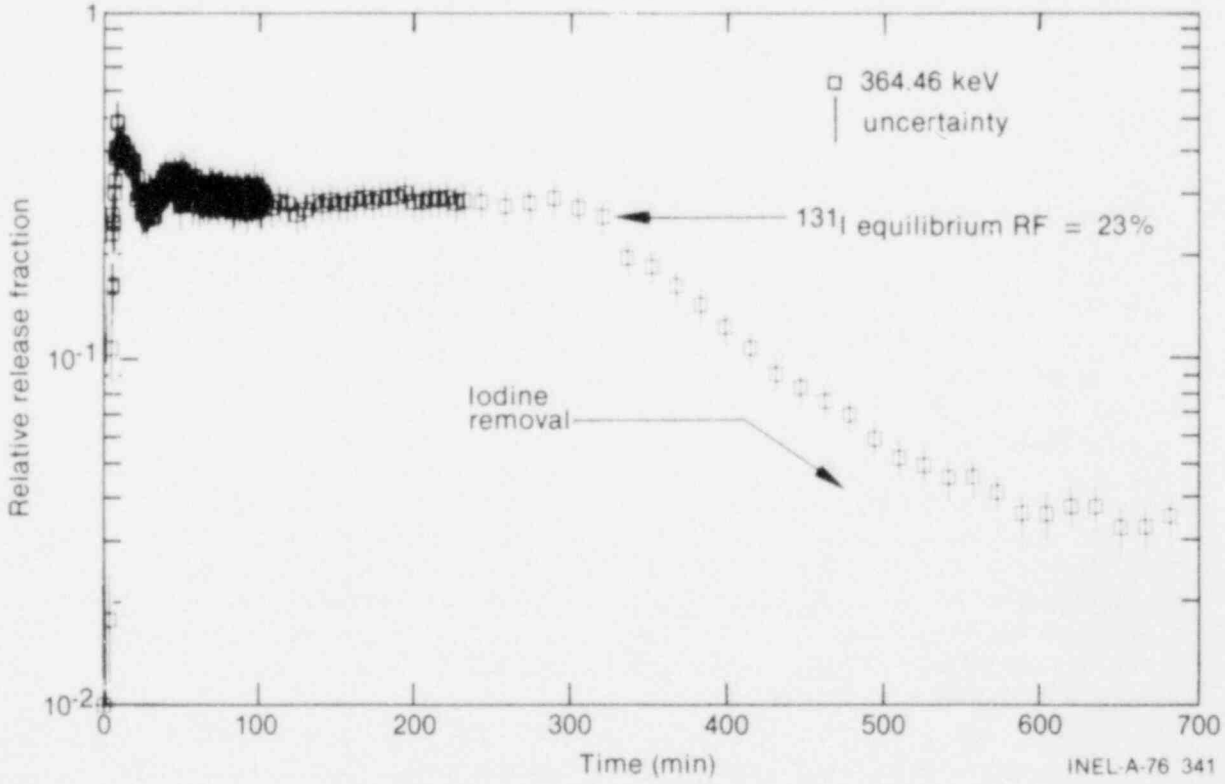

Figure 15. Release fraction history of ^{131}I illustrating rapid removal specific to iodine.

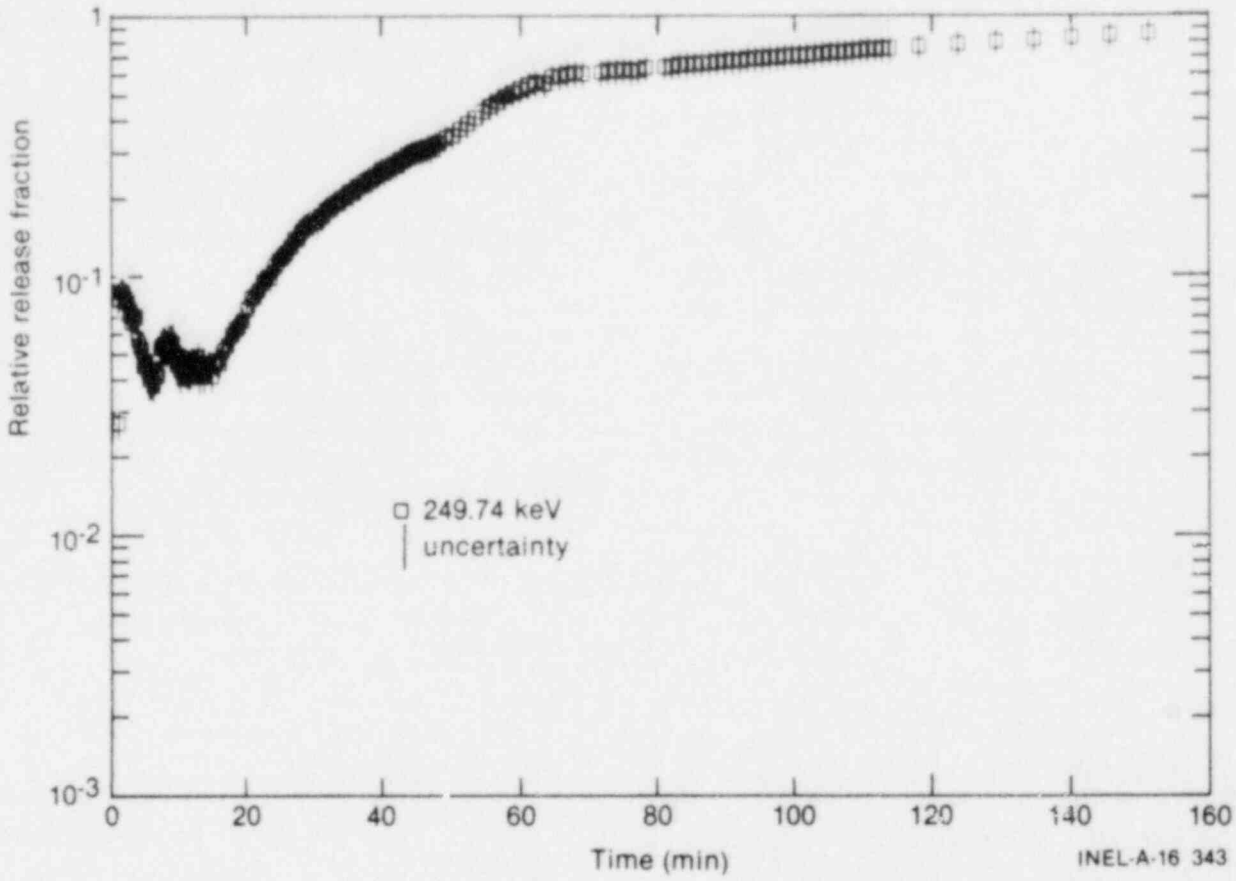

Figure 16. Release fraction history of ^{135}Xe illustrating long-lived source term.

might conceivably be released. It is interesting to compare the recommended release fractions from traditional sources with the results reported here for the PBF tests. Analysis of fission product release usually follows the format presented in the Reactor Safety Study.[1] This format includes a separate treatment of fission product release during four stages of accident severity: gap release, meltdown release, vaporization release, and oxidation release. Table 3 presents a comparison of the recommended values for noble gases, halogens, alkali metals, alkaline earths, and refractory elements taken from the NRC Regulatory Guides,[7,8,9] WASH-1400,[1] and the Three Mile Island (TMI) accident.[6] Also included in Table 3 are the PBF results. The release fractions given in the WASH-1400 column of Table 3 are the values suggested for a meltdown release.

The PBF results for Test PCM-1 tend to agree with the other sources in the catagories of noble gas, alkali metals, and refractory elements. The halogen release fractions in the PBF tests are, however, well below the other reported release fractions. The alkaline earth values are also low, but the alkaline earth results from TMI tend to agree with the PBF data. The ratio of iodine to noble gas release fractions for the TMI accident also agree with the PBF data for the two tests in which fuel powdering but no fuel melting occurred. This supports the conclusion that the TMI core probably experienced fuel powdering, but not a significan. amount of fuel melting. The PBF results for the RIA tests have high values in the alkaline earth and refractory groups, and low values in the halogens. The possible reasons for these differences, which center on fuel powdering and short irradiation, were discussed in the previous section.

Although the fuel in the PBF tests did not experience total meltdown, the release fractions observed are very nearly the same magnitude as the WASH-1400 meltdown release fractions. The

Table 3. A comparison of suggested and reported fission product release fractions

Fission Product Group	NRC Regulatory Guides		WASH 1400	TMI Results	PBF Tests[a]		
	Cladding Rupture	Fuel Melt[b]	Meltdown Release		PCM-1 25% Melt	RIA-ST-1 and RIA-ST-2 No Melt	RIA-ST-4 90% Melt
Noble gases	0.10	1.00	0.87	0.70	0.86 to 1.00	0.15 to 1.00	0.26 to 0.85
Halogens	0.10	0.25	0.88	0.42 to 0.59	0.012 to 0.024	0.21 to 0.62	0.042 to 0.064
Alkali metals	c	c	0.76	0.57 to 0.76	0.02 to 0.90	0.43 to 1.00	0.18 to 0.45
Alkaline earths	c	c	0.10	<0.0007	0.0024 to 0.0075	0.13 to 0.87	0.021 to 0.52
Refractory elements	c	c	0.003	d	0.0019	0.13 to 1.00	0.012 to 1.00

a. Normalized equilibrium release fractions measured in coolant (from Table 2).

b. NRC Regulatory Guides specify that these fractions are assumed to be available for release from containment.

c. The estimated releases of these species are not specified in the NRC Regulatory Guides.

d. None reported.

PBF release fractions are relative numbers and may be artificially high by a factor of two to ten, but it is highly unlikely that they are more conservative than one order of magnitude. Analysis of the posttest loop coolant samples (letdown in temperature and pressure) indicated that the absolute iodine release fractions were approximately 2.6 and 12.7% during Test PCM-1 and the RIA-ST-4 experiment, respectively. These numbers agree to within a factor of three with all of the iodine relative release fractions, and agree almost exactly with the Test PCM-1 results. This suggests that the relative release fractions reported for Test PCM-1 are nearly absolute numbers, and the RIA-ST-4 numbers may be high by a factor of two or three.

The measured relative release fractions for the refractory elements in the RIA tests were approximately two orders of magnitude higher than expected. One possible explanation for this large release may be the extensive fuel fracturing and powdering experienced in the PBF tests. A large fraction of the measured coolant concentrations of fission products may have been associated with these particulates. Accident analyses generally ignore this phenomenon and assume that the worst-case behavior involves loss of coolant, fuel heatup, and melting. However, as demonstrated in the TMI accident and each of the four PBF tests, reactor accidents can involve extensive fuel fragmentation due to coolant injection and quenching of the hot ceramic fuel. This phenomenon produces fuel particulate source terms that may account for transport of a large fraction of fission product activity. Greater attention needs to be given to such fuel fracturing and particulate source terms in accident analyses.

5. CONCLUSIONS

Fission product release from failed fuel has been experimentally measured during PBF Test PCM-1, RIA-ST-1, RIA-ST-2, and RIA-ST-4. Relative fission product concentrations in the PBF coolant loop were determined for a maximum of 20 short-lived fission products per test. Relative release fractions were calculated by comparing integrated coolant activity with fuel rod fission product inventories calculated with the ORIGEN computer code. Plots of isotopic relative release fractions were normalized to provide upper limits for release fractions.

From the comparison (Section 4.4) of PBF normalized release fractions with values suggested in the literature and reported for the TMI accident, it is concluded that:

1. Release fractions of iodine isotopes in the PBF tests that included fuel melting were an order of magnitude lower than the values suggested in the NRC Regulatory Guides and WASH-1400. Iodine release fractions in the PBF tests in which no fuel melting occurred, but in which fuel powdering or desintering did occur, were similar in magnitude to the values suggested in the Regulatory Guides and WASH-1400 for release from molten fuel, and in agreement with the reported TMI accident results.

2. Release fractions of noble gas isotopes in the PBF tests with and without melting were similar to the melt release values suggested in the Regulatory Guides and WASH-1400, and in agreement with the values reported for the TMI accident.

3. Release fractions of some barium and lanthanum isotopes in the PBF tests were approximately two orders of magnitude higher than the values reported for the TMI accident and the melt release values suggested in WASH-1400.

4. Release fractions of cesium and rubidium isotopes in the PBF tests were in agreement with the melt release values suggested in WASH-1400 and the reported TMI accident values.

The isotopic relative release fraction plots generated from this study demonstrate the importance of time-dependent release, precursor influence, and removal processes for evaluating isotopic source terms. Fission product releases measured during the four PBF tests demonstrate that fuel temperatures, fuel powdering or desintering, and the duration of irradiation may create unexplained variations of fission product release within a given chemical species. The fission product source terms associated with fuel fracturing or powdering during quench from high temperatures should be considered in accident analysis. The release fractions from the core to the circulating primary coolant may be much larger during certain accidents than conventional analysis methods would predict. The PBF results displayed much larger release fractions during the RIA tests than might have been predicted by conventional analysis. The larger release fractions may be associated with the unique irradiation conditions that occur during an RIA, but they are probably attributable to the fuel powdering phenomenon observed in the tests.

The uniqueness of the PBF and the FPDS offers an opportunity to analyze the unexplained fission product behavior cited above. Tests dedicated to fission product release definition would help eliminate the complications found in PCM and RIA tests. The effects of fuel temperature and irradiation history prior to failure influence the fission product releases observed in this study. Controlled loop pressure and temperature could demonstrate important fission product transport relationships.

The development of new, up-to-date regulatory guides for accident analysis and plant licensing will depend on accurate information about fission product release during off-normal periods. Fission product behavior modeling and code development require similar information and could eventually be linked to the sophisticated fuel behavior codes to provide a realistic estimate of the source terms and consequences of reactor accidents. Finally, the development of the understanding of fission product behavior could be coupled to modern on-line gamma spectroscopy techniques to aid the development of a fuel condition monitor. Accurate fission product monitoring in nuclear plants would provide a diagnostic tool that could be used by reactor operators to assess fuel conditions during power maneuvers, anticipated transients, and accidents.

6. REFERENCES

1. U. S. Nuclear Regulatory Commission, *Reactor Safety Study: An Assessment of Accident Risks in U. S. Commercial Nuclear Power Plants*, WASH-1400 (NUREG-75/014), October 1975.

2. U. S. Atomic Energy Commission, *The Safety of Nuclear Power Reactors (Light Water Cooled) and Related Facilities*, WASH-1250, July 1973.

3. A. Birkhofer, A. W. Heuser, K. Koeberlein (GfR-Germany), "Assessment of Accident Risks in German Nuclear Power Plants," *Transactions of the American Nuclear Society, 32*, June 1979, pp. 466-467.

4. T. E. Murley, L. S. Tong, G. L. Bennett, *Summary of LWR Safety Research in the USA*, NUREG-0234, May 1977.

5. *Water Reactor Safety Research Program*, NUREG-0006, February 1979.

6. W. N. Bishop et al., "Fission Product Release from the Fuel Following the TMI-2 Accident," *Proceedings of the ANS/ENS Topical Meeting on Thermal Reactor Safety*, CONF-800403, June 1980.

7. "Assumptions Used for Evaluating the Potential Radiological Consequences of a Loss-of-Coolant Accident for Boiling Water Reactors," *NRC Regulatory Guide 1.3*, June 1974.

8. "Assumptions Used for Evaluating the Potential Radiological Consequences of a Loss-of-Coolant Accident for Pressurized Water Reactors," *NRC Regulatory Guide 1.4*, June 1974.

9. "Assumptions Used for Evaluating a Control Rod Ejection Accident for Pressurized Water Reactors," *NRC Regulatory Guide 1.77*, May 1974.

10. R. L. Heath and J. E. Cline, "Effluent Monitoring in Nuclear Plants Using On-Line Gamma-Ray Spectometry," *IEEE Transactions on Nuclear Science, NS-20*, 1, 1973.

11. A. D. Appelhans, A. S. Mehner, W. J. Quapp, "Power Burst Facility Fission Product Detection System," *Transactions of the American Nuclear Society 28*, June 1978 pp. 121-122.

12. D. J. Osetek et al., "The Power Burst Facility Fission Product Detection System," *Review Group Conference on Advanced Instrumentation for Reactor Safety Research*, NUREG/CP-0007, October 1979.

13. J. E. Cline, M. H. Putnam, R. G. Helmer, *GAUSS VI: Computer Program for the Automatic Batch Analysis of Gamma-Ray Spectra from Ge(Li) Spectrometers*, NCR-1113, 1973.

14. M. J. Bell, *ORIGEN - The ORNL Isotope Generation and Depletion Code*, ORNL-4628, 1973.

15. D. T. Sparks and C. J. Stanley, *Power-Cooling-Mismatch Test Series, Test PCM-1 Fuel Rod Behavior Report*, NUREG/CR-0907, TREE-1374, August 1979.

16. B. A. Cook, *Fuel Rod Material Behavior During Test PCM-1*, NUREG/CR-0757, TREE-1333, June 1979.

17. D. E. Thornton and D. H. Schwieder, *Experiment Data Report for Test PCM-1 (Power-Cooling-Mismatch Test Series)*, NUREG/CR-0292, TREE-1233, September 1978.

18. C. L. Zimmerman et al., *Experiment Data Report for Test RIA-ST (Reactivity Initiated Accident Test Series)*, NUREG/CR-0473, TREE-1235, March 1979.

19. R. S. Semken et al., *Reactivity Initiated Accident Test Series RIA Scoping Tests Fuel Behavior Report*, NUREG/CR-1360, EGG-2024, April 1980.

20. M. S. El-Genk and R. L. Moore, *A Study of Molten Debris Freezing and Wall Erosion in the RIA-ST-4 Experiment*, NUREG/CR-1072, EGG-2030, April 1980.